

Geology of the Chuquicamata Mine: A Progress Report

GUILLERMO OSSANDÓN C.,

CODELCO-Chile, Gerencia Exploraciones, Santiago, Chile

ROBERTO FRÉRAUT C.,

CODELCO-Chile, Superintendencia Geología, Chuquicamata, Chile

LEWIS B. GUSTAFSON,[†]

5320 Cross Creek Lane, Reno, Nevada

DARRYL D. LINDSAY,

SRK Consultores, Santiago, Chile

AND MARCOS ZENTILLI

Department of Earth Sciences, Dalhousie University, Halifax, Nova Scotia, Canada B3H 3J5

Abstract

Chuquicamata, in northern Chile, is the world's greatest copper orebody. It was controlled, from the initial intrusions (probably at 36–33 Ma) through mineralization (last major hydrothermal event at 31 Ma) to post-mineral brecciation and offset, by the West fault system. East porphyry, West porphyry, Banco porphyry, and Fine Texture porphyry make up the Chuqui Porphyry Complex. East porphyry, the dominant host rock, has a coarse, hypidiomorphic-granular texture. Intrusive contacts between most porphyries have not been found, but early ductile deformation, subsequent pervasive cataclastic deformation, and faulting affects all of the rocks and makes recognition of intrusive contacts very difficult.

Potassic alteration affects all porphyries, comprises partial K feldspar and albite replacement of plagioclase, and more widespread biotite replacement of hornblende, with igneous texture largely preserved. It is accompanied by granular quartz and quartz-K feldspar veinlets, which contain only trace disseminated chalcopryrite ± bornite remains from this early stage. Fine-grained quartz-K feldspar alteration, with destruction of biotite and apparently following albitization of plagioclase, accompanies strongest cataclastic deformation and destruction of igneous texture. A band of quartz-K feldspar alteration, up to 200 m wide and 1,500 m long, lies along the southward extension of Banco porphyry dikes and is the locus of the bornite-digenite center of the sulfide zoning pattern. This passes east through chalcopryrite-bornite to chalcopryrite-pyrite as sulfide abundance fades out. Sulfides in quartz-K feldspar alteration are abundant only where there is intense crackle brecciation. Propylitic alteration is superimposed on biotitic alteration at the eastern edge of the deposit, but there is no pyritic fringe. Westward, this zoning is interrupted by the superposition of pyritic main-stage veins with pervasive quartz-sericite. Veins of quartz-molybdenite, up to 5 m wide and cutting all porphyries, were emplaced between the early and the main stages. These veins and early-stage quartz veins are commonly segmented and sheared, with fine recrystallization of quartz that eliminates all original fluid inclusions. It is not clear whether quartz-K feldspar alteration was formed later or earlier than quartz-molybdenite veins.

Main-stage veins were focused along a structural zone adjacent to the West fault. This stage is distinctly younger than early-stage mineralization, although it occupies many of the same structures and may involve massive remobilization of earlier mineralization. It may represent a more brittle and much shallower environment, which followed significant erosion of the upper parts of the early mineralization system. Main-stage veins with quartz, pyrite, chalcopryrite, and bornite were formed during dextral shear of the West fault system. The last mineralization of the main stage was enargite, digenite, covellite, pyrite, and minor coarse sphalerite, along with sericite, and locally alunite but only local traces of pyrophyllite and dickite. Some northwest enargite veins were apparently opened after the sense of shear on the West fault system changed to sinistral. Vein and veinlet filling faults and fault-related shatter zones contain the overwhelming proportion of copper at Chuquicamata in all alteration zones and assemblages, including pyrite-free early-stage assemblages. Practically all of these fractures have been opened and mineralized more than once.

A still poorly understood late stage formed digenite with relatively coarse grained covellite from deep in the sericitic zone and flaring upward and outward under what became the supergene chalcocite enrichment blanket. The presence of associated anhydrite, typical also of earlier stages but largely leached or hydrated to gypsum by later supergene action, proves this is not supergene covellite, but it is otherwise very difficult to distinguish from supergene covellite. Rims of sphalerite on primary sulfides, almost invariably with inner rims of coarse-grained covellite and/or digenite, occur below the chalcocite blanket from which Zn has been leached.

[†] Corresponding author: e-mail, lgustaf685@aol.com

The sphalerite rims are interpreted by most as supergene, but the close association with apparently late hydrothermal covellite-digenite and their absence in all other porphyry copper deposits suggests they too may be hydrothermal.

A partially preserved leached capping and oxide copper ore, replacing an upper chalcocite blanket, overlies a high-grade supergene chalcocite body that extends up to 800 m in depth in the zone of fault brecciation and pervasive main-stage sericitic alteration. Some leached copper moved laterally to form exotic copper oxides and silicate in adjacent gravels. Continued movement on the West fault produced a wide zone of brecciation and major displacements of mineralized rock. Net sinistral displacement of about 35 km is indicated by regional mapping, but the details of how much of each stage of mineralization was displaced and how far on which splits of the fault are not well understood. The uniqueness of Chuquicamata is due to its intimate and complex relationship with active regional faulting and to superposition of at least two distinct periods of mineralization.

Introduction

CHUQUICAMATA lies at about the 2,800-m elevation in the Atacama Desert of northern Chile, some 240 km northeast of Antofagasta (22° 17.5' S, 68° 54.5' W). Outcropping high-grade copper oxide was first worked in a small way by both the Incas and Spanish explorers (Miller and Singewald, 1919). From 1879 to 1912, Chilean and English companies worked narrow but rich veins of brochantite overlying enargite and chalcocite with pyrite and quartz. Their underground workings followed a N 10° E structural zone, extensions of the Panizo fissure in figure 1 of López (1939), which is today scarcely recognizable in the upper to middle benches in the northeast portion of the pit. In 1915, Chile Exploration Co., operating arm of the Guggenheim's Chile Copper Co., initiated open-pit mining on disseminated oxide ore averaging 1.89 percent Cu. Production started at 10,000 short tons per day from what was initially estimated at 96 million short tons of 2.41 percent Cu, but by year end 1916, proven and probable ore reserves had increased to 700 million metric tons (Mt) of 2.12 percent Cu (Chile Copper Co., 1917). Anaconda Copper Mining Co. purchased the property from the Guggenheims in 1923 and subsequently managed 48 yr of continually expanding operation. Early descriptions of the geology were published by Taylor (1935), López (1939, 1942), and Perry (1952). These publications summarize geologic mapping by Anaconda mine geologists and internal reports by W. Lindgren (1917), R.H. Sales (1930), W. March (1939), and L.G. Zeihen (1952). Jarrell (1944) described the oxide and enriched sulfide ores and interpreted supergene processes on the basis of experimental chemistry. Production increased and shifted from dominantly oxide to dominantly sulfide ores in the 1950s as the pit deepened. Oxide production was extended by the accidental discovery in 1957 of the Exótica deposit (now South mine) beneath the oxide tailings dump, and its subsequent systematic exploration and development in the 1960s. It is still the largest exotic copper deposit known. Anaconda built a major mining and metallurgical complex, including oxide plant, concentrator, smelter, refinery, and town close to the mine, and a power plant at Tocopilla on the coast, and Chuquicamata became the world's largest copper producer. Geologic documentation continued in the form of routine but detailed Anaconda-style 1:400 scale mapping by mine staff, supported periodically by the Anaconda geologic laboratories at Butte and El Salvador. This work was reported only in unpublished internal reports, most notably by G. Watterman (1951), R. Applegate (1960), J. Hunt (1962), B. Thompson (1964), and H. Langerfeldt (1964), and a Ph.D. thesis by Renzetti (1957).

In 1971, the mine was nationalized and management and operation were taken over by the Corporación Nacional del Cobre-Chile (CODELCO). Emphasis on production and major drilling campaigns followed, extending knowledge of the orebody to 1 km below the premine surface and furthering exploration of the Pampa Norte deposit. This deposit was discovered by Anaconda in the 1960s and was later developed by CODELCO as the Radomiro Tomic mine. In the early 1970s, J. Ambrus and his group generated the first comprehensive geologic model for Chuqui, considering factors such as multiple overprint events, definition of secondary enrichment zones, definition of primary ores and relationships with alteration phases, and potential orebody offset; all of them considered in a genetic proposal for the orebody. Computerization of most aspects of ore reserve calculation, grade control, mine planning, etc. was accomplished. The evolving status of geologic knowledge was recorded by numerous undergraduate theses ("memoria") and Ph.D. theses by Ambrus (1979) and Soto (1979). Among the few published reports are those of Alvarez et al. (1980) and Alvarez and Flores (1985). By 1993 it was clear that revision of the geologic model used by the mine for mine planning and operating control was long overdue, and a major effort was initiated to update all aspects. Some 2,300 diamond drill holes were relogged and/or reinterpreted, logging and pit mapping criteria were revised, the portions of the pit within the orebody were remapped to completely revise the geologic models for structure, mineralization, and alteration, and special studies were undertaken to define the distribution of Mo, As, Zn, and metallurgical parameters within the orebody. Mine staff was supplemented by several experienced consultants to accomplish this huge task in just over 2 yr. Over the past few years, extensive 1:50,000 scale quadrangle mapping by geologists of Servicio Nacional de Geología y Minería (SERNAGEOMIN), sponsored by CODELCO, has greatly increased our understanding of the regionally important Domeyko fault system (Tomlinson and Blanco, 1997).

The results of these combined efforts were the focus of a day-long symposium sponsored by the Society of Economic Geologists at the Eighth Chilean Geological Congress in 1997 (vol. III, p. 1871–1965). They have been reported in the various published and unpublished papers cited herein and are summarized in this and accompanying papers. The symposium covered many operational as well as geologic aspects of the Chuquicamata district, which comprises ore deposits strung out over nearly 30 km, from MM (Mansa Mina) on the south to Radomiro Tomic on the north (Fig. 1). Along with related exotic copper mineralization, both north and south of the Chuquicamata open pit, this cluster of deposits

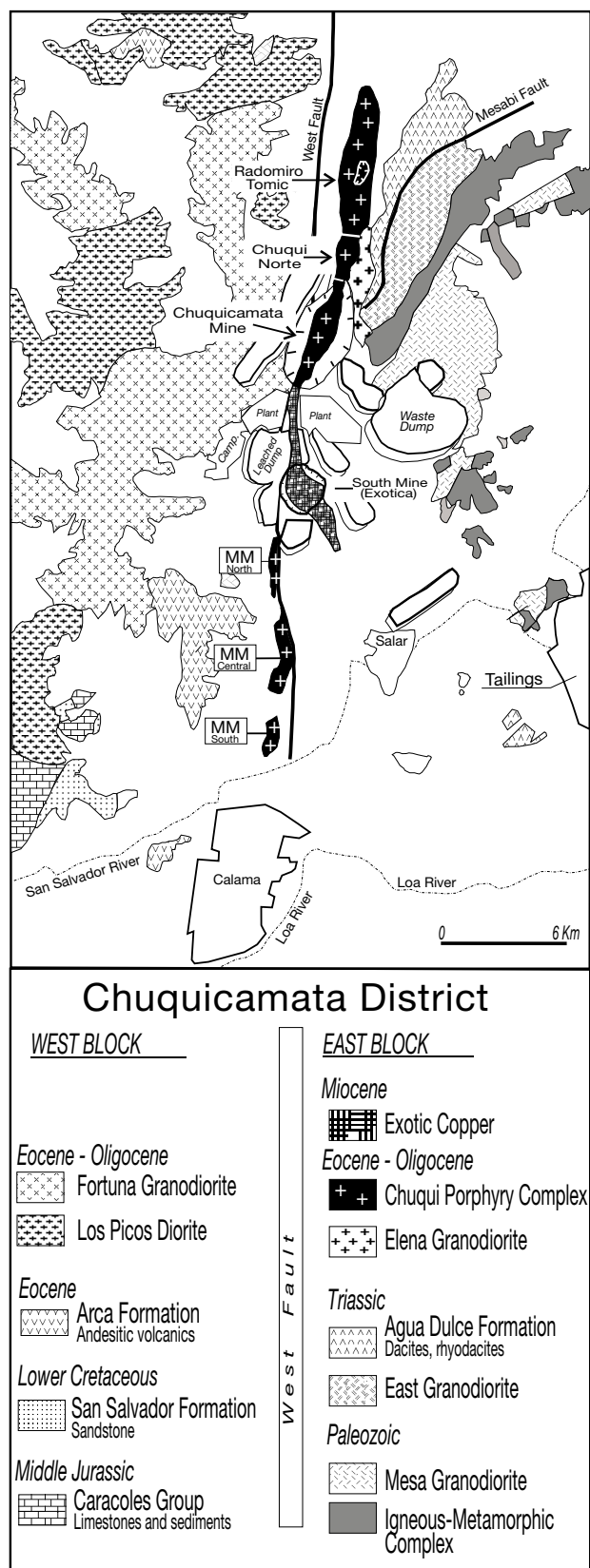


FIG. 1. The Chuquicamata district, showing major geologic units and location of mines. Geology is modified from G. Chong and R. Pardo, unpublished map (1997). The Chuquicamata mine is at 22°17.5' S, 68°54.5' W (UTM E510350, N7535600).

represents a concentration of recovered and mineable copper of nearly 90 Mt (Ossandón and Zentilli, 1997).

Production and reserves

Ossandón and Zentilli (1997; Table 1) list total resources—historic and annual production for the Chuquicamata district as of 1997. Two thousand and thirty-five million metric tons (2,035 Mt) of ore, averaging 1.54 percent Cu has been mined from the Chuquicamata orebody, plus 120 Mt of 1.25 percent Cu from the South mine. A resource of some 6,450 Mt at 0.55 percent Cu remains in the main orebody, plus 190 Mt of 1.12 percent Cu remains in the South mine. If resources in the MM project to the south and the Radomiro Tomic mine to the north (Fig. 1) are included, the combined resource still to be mined plus past production is 11.4 billion tons of 0.76 percent Cu, rivaled only by El Teniente and Andina-Disputada as the greatest copper mining district in the world. In 1997, the combined production from the Chuquicamata and Exótica orebodies was 644,000 t of fine copper.

Geologic Setting

Chuquicamata is in the Precordillera of northern Chile, which is parallel and west of the volcanoes that form the modern continental arc of the Andean Cordillera. It is related to Eocene-early Oligocene porphyritic intrusions that occur within the middle to late Cenozoic Domeyko fault system. The setting is similar to that of several Eocene and Oligocene porphyry copper deposits in the belt stretching from at least Potrerillos to Quebrada Blanca, but Chuquicamata is the most closely related in space and time to this fault system.

Pre-Oligocene rocks

In the Chuquicamata district, the oldest rocks occur in a north-northeast-trending belt of Paleozoic metasedimentary and metaplutonic rocks, which are exposed within the South mine pit and within a kilometer east of the Chuquicamata pit (Fig. 1). These rocks include gneissic granite, metadiorite, quartz diorite, and minor tonalite recrystallized in varying degrees to amphibolite (A. Tomlinson, writ. commun., 1999). Pervasive chlorite-epidote-calcite alteration in the metadioritic rocks is so widespread that it was interpreted by Ambrus (1979) as retrograde regional metamorphism rather than propylitic alteration related to the orebodies. Dioritic rocks intrude the Mesa Granite, a pink microcline granite with locally developed weak to moderate gneissic fabric. This granite is also recognized in the Sierra Limón Verde, south of Calama, where it is dated at late Carboniferous (Marinovic and Lahsen, 1984). East Granodiorite intrudes the west edge of the metaplutonic complex and extends at least 9 km north-northeast from the southeast edge of the Chuqui pit along the crest of the Chuquicamata Hills. It is medium to coarse equigranular texture, with plagioclase, microperthitic K feldspar, quartz, biotite, and hornblende. U-Pb zircon dating indicates a Middle Triassic age (A. Tomlinson, writ. commun., 1999). Local alteration to albite-chlorite-magnetite and sericite-clay is ascribed to the influence of the Chuquicamata porphyries (Ambrus, 1979).

In the Sierra Limón Verde, these crystalline rocks are unconformably overlain by a volcanic and sedimentary sequence of Mesozoic age. At its base this sequence consists of continental

TABLE 1. Geologic Resources and Production, Chuquicamata District (cutoff grade 0.2% Cu)

Deposit		Resources ¹		Mined out	
		Million tons	Cu (%)	Million tons Cu	Million tons Cu (%)
Chuquicamata		8485	0.79	67.03	2035
	Chuqui oxides	506	1.56	506	1.56
	North zone oxides	350	0.43		
	Enriched sulfides	2229	1.41		1529 ²
	Primary sulfides	5400	0.48		1.53
Exótica (South mine)	Oxides	310	1.17	3.63	120
Radomiro Tomic		2330	0.59	13.75	
	Oxides	850	0.62		
	Enriched sulfides	180	0.93		
	Primary sulfides	1300	0.53		
Proyecto MM		325	0.96	3.12	
	Oxides	25	1.11		
	Sulfides	300	0.95		
Total		11450	0.76	87.02	2155
	Oxides	2041	0.91	18.57	625
	Enriched sulfides	2409	1.37	33.00	1529 ²
	Primary sulfides	7000	0.51	35.70	1.53

¹ Includes historical production
² Includes primary sulfides

Mine production		Million tons		Grade Cu (%)	Thousand tons Cu
Year 1997					
Concentrator	Chuquicamata	Sulfides	53	1.05	481
Hydrometallurgical					314
	Exótica (South mine)	Oxides	10	1.2	84
	Chuquicamata	Low-grade sulfide ore	15	0.36	13
		Old leach tailings			67
	Radomiro Tomic	Oxides			150
Total fine copper					794

facies conglomerate, sandstone, and andesitic and dacitic lava, breccia, and tuff of presumed Late Triassic age (Lira, 1989; Mpodozis et al., 1993). This is gradationally overlain by a transgressive marine sequence of Jurassic shale, sandstone, and limestone. In the Chuquicamata Hills, equivalent Mesozoic rocks are frequently in fault contact with the basement rocks or the contact is too poorly exposed to determine its nature (A. Tomlinson, writ. commun., 1999). Here andesitic volcanic rocks are the dominant Mesozoic lithology, but continental sandstone units crop out on the north flank of the Chuquicamata Hills. Marine limestone and calcareous shale occur as fault slivers along the Mesabi fault from the north end of the hills to the east edge of the pit. In the pit, the sedimentary units consist of calcareous, fine-grained sedimentary rocks that are intruded and contact metamorphosed by East porphyry of the Chuqui Porphyry Complex (Lindsay, 1998).

Eocene-Oligocene intrusions

The major postmineral West fault separates the porphyritic rocks in the Chuquicamata pit, with the dominantly barren

Fortuna Complex to the west and the intensely mineralized Chuqui Porphyry Complex to the east. Rocks with textures essentially identical to those of the Chuqui Porphyry Complex extend northward at least 9 km through the Radomiro Tomic mine (Cuadra et al., 1997; Cuadra and Rojas, 2001).

Structure

The fault separating the two halves of the Chuquicamata pit is the West fault, the famous West Fissure of early literature (Fig. 2). It is a major strand of the West fault system (Tomlinson and Blanco, 1997), as the portion of the Domeyko fault system north of Calama is now called. This is a regional structural zone extending several hundred kilometers in northern Chile. It is interpreted as a Cenozoic age, arc-parallel set of transcurrent and reverse faults. Having fascinated explorationists for decades, it has recently been the focus of several studies (e.g., Maksaev and Zentilli, 1988, 1999; Maksaev, 1990; Reutter et al., 1991; Lindsay et al., 1995; Tomlinson and Blanco, 1997). Just north of the Chuqui pit, the zone is 5 km wide, from the Tetera fault on the west to the Mesabi

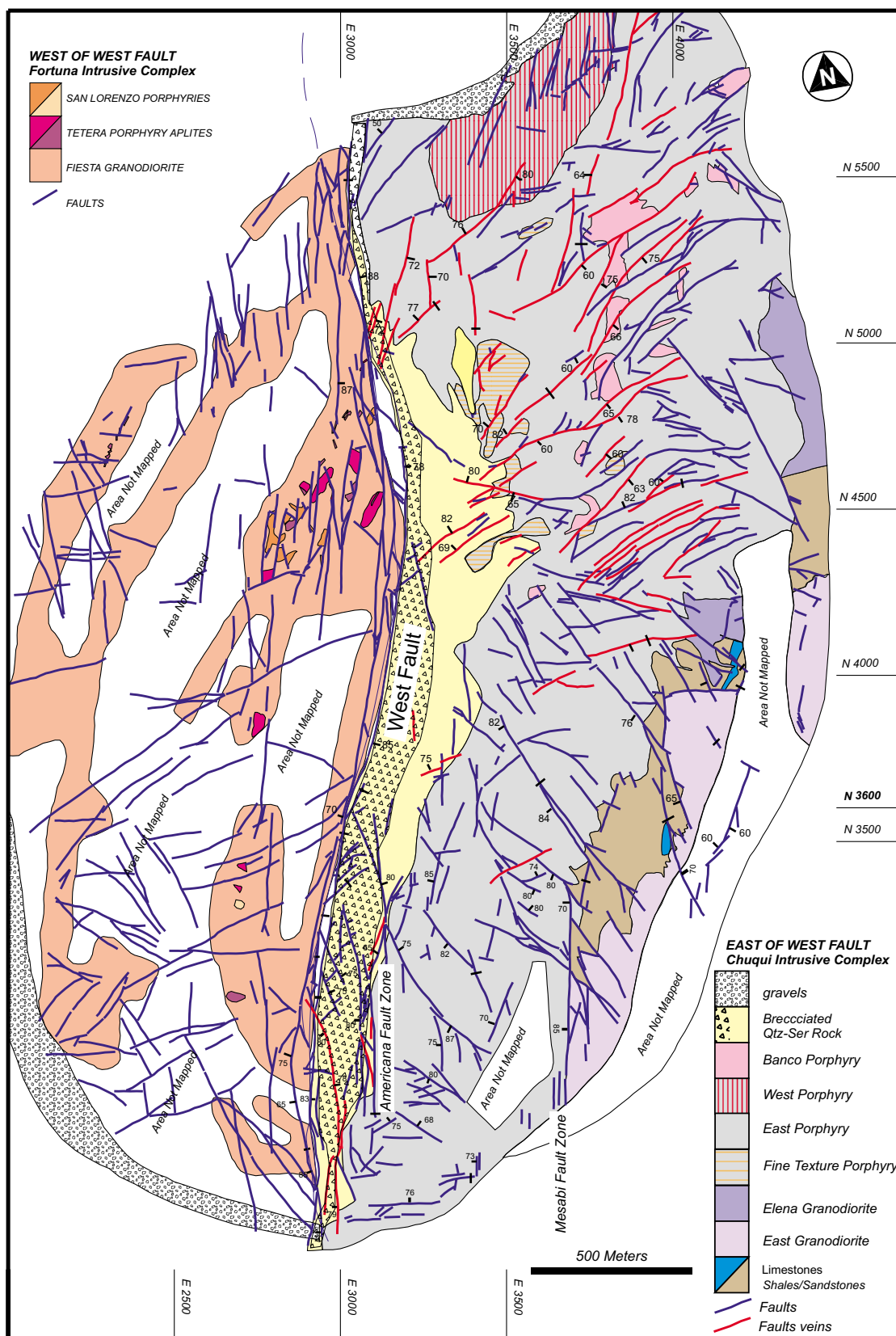
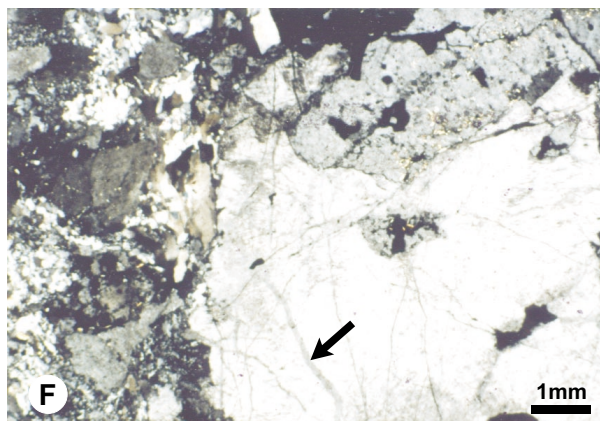
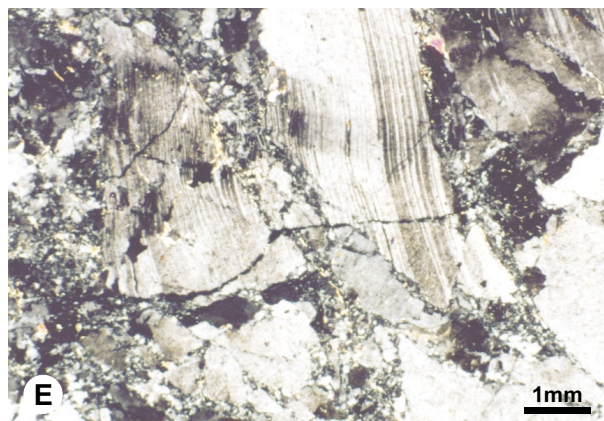
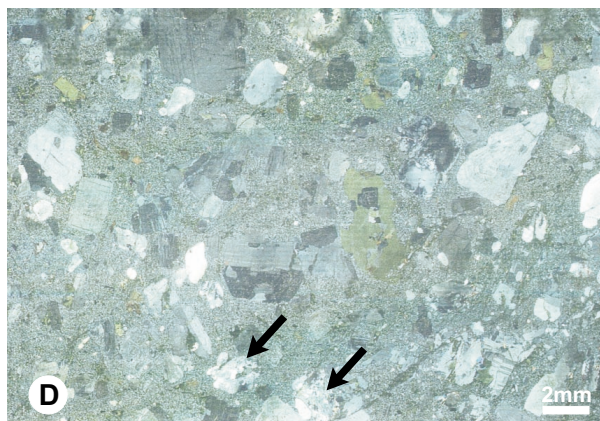
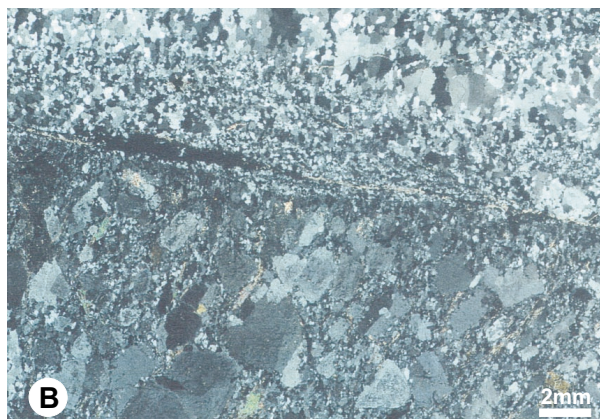
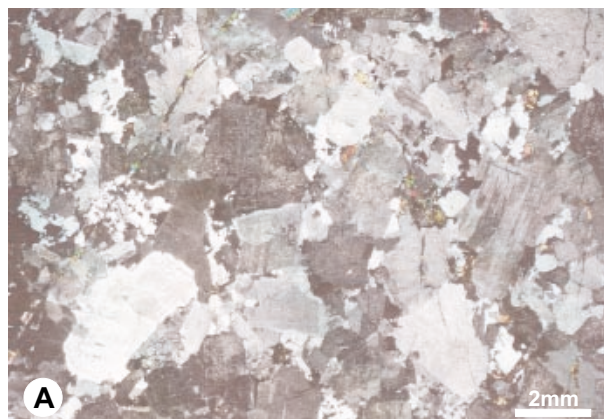


FIG. 2. Rock types and major structures exposed in the Chuquicamata open pit in 1998. See 500-m local coordinates for scale. Note true north is 10° west of mine north in this and all other pit maps. Bottom bench is at 2,944 m elev, top bench is at 2,944 m. Only those structures continuous over 3 benches (39 m) are shown. Faults in area not mapped are interpreted from rock mechanics data only (Torres et al., 1997).



fault on the East. Dilles et al. (1997) and Tomlinson and Blanco (1997) describe the evolution of the West fault system. It has been active prior to intrusion of the Chuqui Porphyry Complex until after 16 Ma, changing sense of movement at least twice. It has had a critical control on the emplacement of the host intrusions, formation of mineralized structures, and postmineral displacement of the orebodies.

Rock Types

Fortuna Intrusive Complex

The pattern of mappable rock types exposed in the pit is shown in Figure 2. The Fortuna Intrusive Complex adjacent to the open pit contains only low-grade mineralization and has been structurally juxtaposed against the intensely mineralized Chuqui Porphyry Complex by large-scale, postmineral movement on the West fault—documented by Dilles et al. (1997), Tomlinson and Blanco (1997), and previous workers. Lithologic units shown within the Fortuna Intrusive Complex (Fig. 2) were mapped by Lindsay (1995, unpub. report) and Dilles and are described by Dilles et al. (1997). The volumetrically dominant Fiesta Granodiorite phase of the Fortuna Intrusive Complex is intruded by small irregular bodies of San Lorenzo granodioritic porphyry and minor Tetera aplite porphyry. Fiesta Granodiorite is weakly mineralized with copper oxides in the uppermost northwestern benches of the pit and with sulfides only near contacts of the San Lorenzo porphyries. Mineralization in these porphyries and at contact zones comprises weak chalcopyrite-(bornite) dissemination and veinlets, minor chalcopyrite-magnetite veinlets, and molybdenite on fractures, associated with partial biotite replacement of hornblende. Rock west of the West fault is shipped to the waste dumps and is mapped only for slope stability purposes.

Pre-Chuqui porphyry intrusions

On the eastern margin of the pit are exposed the Elena and East Granodiorites, both intruding metasedimentary rocks that were originally shale and sandstone with minor limestone. Whereas the East Granodiorite is texturally distinctive and clearly older, Elena is mineralogically and texturally similar to the East porphyry. Contacts are obscured, but radiometric dating of the Elena Granodiorite indicates a Jurassic to

Early Cretaceous age: Pb-alpha dating of zircon indicates an age of 146 ± 15 Ma, and K-Ar dating in biotite indicates an age of 122 ± 3.8 Ma (Ambrus, 1979, table 7). All of these rocks at the east edge of the pit are essentially barren of mineralization and practically all recent geologic effort has been concentrated in and immediately adjacent to the orebody, which extends roughly 800 to 1,200 m eastward from the West fault.

Chuqui Porphyry Complex

Practically the entire Chuquicamata orebody is hosted by the Chuqui Porphyry Complex, made up of East, Fine Texture, West, and Banco porphyries (Fig. 2). Each of these contains, in their freshest state, plagioclase, quartz, K feldspar, biotite, and hornblende with accessory sphene and magnetite. Textures vary widely, and practically all exposures are affected by some degree of hydrothermal alteration and pervasive cataclastic deformation. Despite years of detailed mapping and special studies to find intrusive contacts and define temporal relationships between intrusion and alteration-mineralization, sharp intrusive contacts have only been seen between the East and Banco porphyries.

The largest and presumably the oldest intrusion is the East porphyry. It is hypidiomorphic-granular texture (Fig. 3A), with euhedral plagioclase (avg >2 mm), biotite, hornblende, (altered to biotite), and locally K feldspar in a matrix of quartz, K feldspar, and biotite. There is no euhedral quartz, but commonly elongated polycrystalline and strained quartz blebs are prevalent and are probably deformed phenocrysts. The West porphyry has similar phenocrysts, though slightly finer grained (avg plagioclase <2 mm) and with quartz eyes common, in an aplitic groundmass of much finer equigranular quartz, K feldspar, and biotite. In the north central portion of the pit, euhedral K feldspar megacrysts (to 2 cm) occur in both porphyries. Although considered by some as metasomatic, Langerfeld (unpub. report, 1964) showed the common occurrence of plagioclase inclusions oriented along growth zones and interpreted them as magmatic features. The abundance and coarseness of aplitic groundmass and matrix in these porphyries vary in an apparently gradational manner near their poorly defined contact (Hunt, unpub. report, 1962), reminiscent of textural variation within the single intrusive unit L porphyry at El Salvador (Gustafson and Hunt, 1975),

FIG. 3. A. East porphyry, with coarse-grained interstitial quartz and K feldspar; potassic alteration with K feldspar veinlets in plagioclase, and biotite after hornblende (not shown); weak deformation with recrystallization of quartz (arrow). No K feldspar megacrysts in this sample. OX1070, D2 bench, 3934N-3881E. B. West porphyry, with aplitic groundmass; potassic alteration and disseminated bornite-chalcopyrite; foliated by weak noncataclastic deformation and recrystallization; early granular quartz-K feldspar veinlet (top half) is perpendicular to foliation in porphyry; vein has K feldspar alteration halo, disseminated molybdenite-chalcopyrite, and is recrystallized by shearing. J1C, J1 bench, 5080N-3500E. C. Sharp intrusive contact East porphyry with Banco porphyry (right); Banco has relatively sparse plagioclase and biotite phenocrysts in characteristic matrix of <1 -mm plagioclase with finer granular quartz and K feldspar. OX1104, location unknown. D. Small dike of porphyry with aplitic groundmass, phenocrysts of subhedral K feldspar (right center, stained yellow, with included plagioclase), biotite, and subhedral quartz phenocrysts (recrystallized, arrows); it intrudes much more deformed East porphyry, possibly being much younger and may be related to dacite dikes at the MM deposit. D3619-684.2, 3799N, 3257E, 1,770-m elevation. A.-D. Color copier print with crossed-polarized sheet. E. Quartz-K feldspar alteration; pervasive albitization of plagioclase and strong cataclastic deformation of East porphyry, with lacing streaks of very fine grained quartz-K feldspar; high-birefringent sericite; D2743-138.3 m. F. Quartz-K feldspar alteration, foliated with extreme texture obliteration in East porphyry; K-feldspar megacryst, which is relatively resistant to cataclastic deformation; East porphyry. D2743-155.2 m. E.-F. Transmitted light, crossed polars. G. Quartz-K feldspar alteration, foliated with extreme texture obliteration in East porphyry; K-feldspar stained yellow; opaques are bornite-digenite. D3226-383.4 m. Plain transmitted light. H. Breccia and crackle filling bornite-digenite-chalcopyrite in quartz-K feldspar altered East porphyry; most feldspar altered here to green sericite, but no pyrite. D3758-261 m.

leaving their identification as separate intrusions in doubt. Locally both porphyries are weakly foliated, even where they lack cataclastic deformation (Fig. 3B), indicating plastic deformation, possibly during intrusion and crystallization.

Banco porphyry is finer grained and more porphyritic than East porphyry, which it intrudes (Fig. 3C). It differs from West porphyry in having an abundance of small plagioclase crystals in the aplitic groundmass. Its texture is also variable, including local K feldspar megacrysts. The Fine Texture porphyry in Figure 2 is distinctly finer grained than normal East porphyry but has a hypidiomorphic-granular texture. Contacts with East porphyry may be abrupt but usually faulted. These occurrences in the pit may correlate with Banco porphyry intersected in drill holes below, and both rock types may be closely related. Most such dikes have been so overprinted by quartz-sericite alteration that their identification is very difficult. As is the case for Banco porphyry, no definitive age relationships (i.e., truncated quartz veins) have been seen at the contacts with Fine Texture porphyry, and megascopically at least both porphyries seem to have been affected by all of the same stages of alteration and mineralization as the East porphyry.

Figure 3D shows a <8-cm-wide dike in East porphyry but which lacks the pervasive cataclastic deformation of the host rock. The texture looks like West porphyry, but it occurs 1,800 m south-southeast of West porphyry (3700 N, 3257 E, 1,770 m elev). Because it is much less altered and deformed, it appears to be much younger than other intrusions in the deposit and is more probably related to Dacite porphyry dikes seen in the MM deposit some 12 km to the south. No other such unaltered dikes have been recognized at Chuquicamata, but this may be the only evidence of intrusion contemporaneous with the main-stage of alteration and mineralization.

Structural Controls

A critical control on events at Chuquicamata, from initial emplacement of the porphyries to metal distribution and slope stability in the present-day pit, has been its dynamic setting within the West fault system (Tomlinson and Blanco, 1997). The various vein systems were formed during an early period of dextral shear developed between the Mesabi fault on the east and a western fault that has probably been displaced by or evolved into the younger West fault. Subsequent reversal of movement to sinistral shear, focused here in a much narrower zone that now runs through the center of the open pit, produced the postmineral offset on the West fault. The evolution of the shear system from ductile to brittle and

its control on mineralization in the deposit have been described by Lindsay et al. (1995), Rojas and Lindsay (1997), and Lindsay (1998).

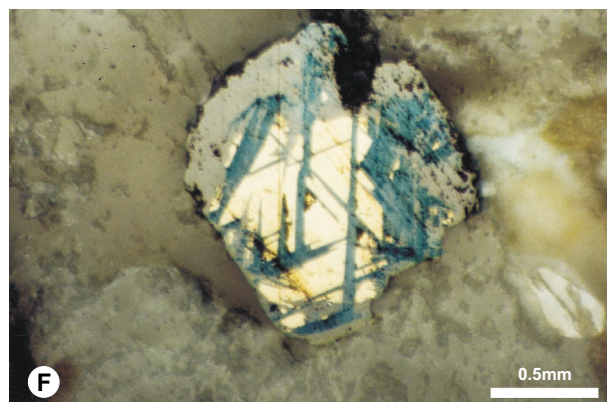
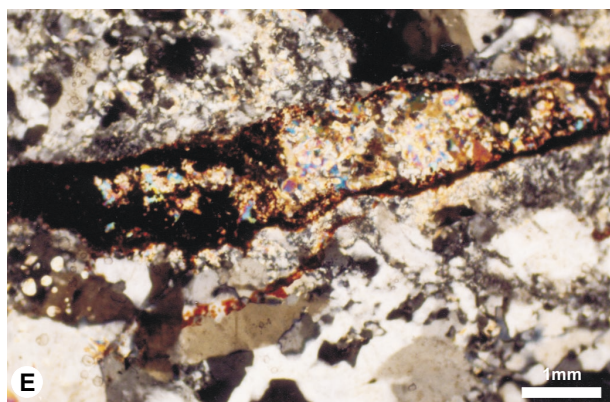
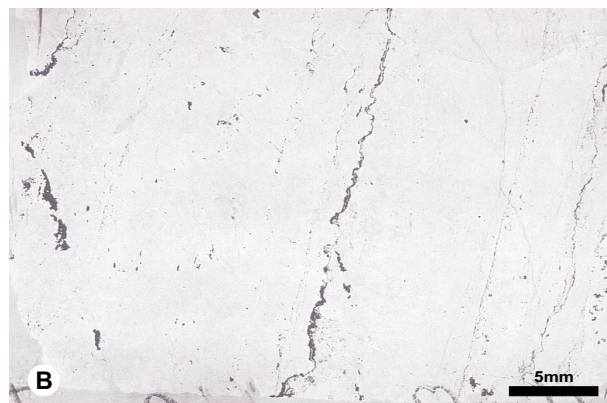
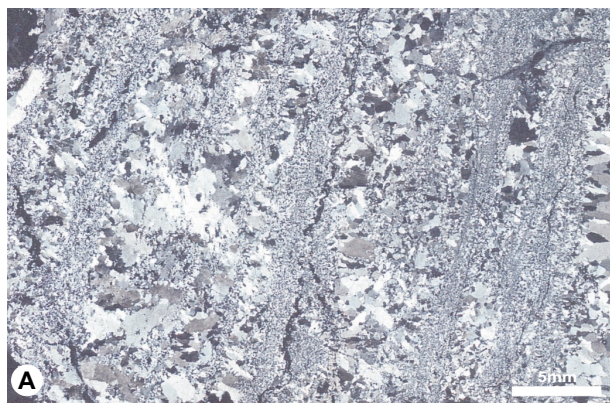
Early ductile deformation

Emplacement of the Chuqui Porphyry Complex was accompanied by and probably facilitated by ductile deformation. At the east edge of the pit, apophyses of East porphyry locally truncate ductile deformation fabrics in the metasedimentary units and Elena Granodiorite, which show a dextral sense of shear in the Mesabi fault zone. In turn, East porphyry contains mylonitic zones that show dextral shear (Lindsay et al., 1995). Most of these zones are parallel to the steeply dipping Mesabi fault, but others in the upper northeastern sector of the pit are reverse faults, which display flat dips to the northeast (Rojas and Lindsay, 1997; Lindsay, 1998). Porphyry texture is completely destroyed in these discrete mylonitic zones. Furthermore, there are large volumes of East and West porphyries with reduced biotite content but with texture largely preserved, where clear foliation and lineation are accompanied by pervasive cataclastic features visible in thin section (see previous discussion and Fig. 3E-G). Pervasive cataclastic deformation probably spanned the extended transition between ductile and brittle and continued throughout at least the early period of alteration and mineralization. It is probably responsible for obliteration of any intrusive contacts that may have existed between the East and West porphyries.

Veins

A large proportion of the copper at Chuquicamata occurs in veins and veinlets filling faults and fault-related shatter zones. Practically all of these fractures in the main orebody have been opened and mineralized more than once, with truncation and superposition of mineral assemblages, seriously complicating the construction of an evolutionary sequence of structure and mineralization. There have been several vein sequences proposed (G. Waterman, unpub. report, 1951; Ambrus, 1979; Lindsay et al., 1995; Lindsay, 1998), which are generally in agreement. Early-stage veinlets of quartz and quartz-K feldspar contain no or only very minor sulfide. These veinlets are cut by more continuous quartz veins, to 5 cm wide, containing minor molybdenite and traces of chalcocopyrite (Fig. 3B, top). Large banded quartz veins, known as blue veins, are typically 1 m or more in width, contain abundant molybdenite, and truncate the previous veins (Fig. 4A and B). These veins are commonly surrounded by sericitic

FIG. 4. A. Quartz-molybdenite vein with coarse texture recrystallized in shear bands parallel walls; from the 30-cm-wide blue vein. Chuqui Mo D; K1 bench, 4970N-3480E. Color copier print with crossed-polarized sheet. B. Same as A but without polarized sheet; fine crystalline disseminated and coarse smear molybdenite in stylolites parallel walls; coarse opaques in discordant fractures are digenite-bornite-pyrite. C. Quartz-molybdenite vein cut by main-stage barren pyrite veinlet (arrow), in turn offset by veinlets of digenite-bornite-pyrite. D3539-736.5 m. D. Main-stage pyrite-quartz-enargite-chalcocite-sphalerite vein (black), 10 cm with ± 1.5 -m sericitic halo (gray) merged with halos of other smaller veins; in kaolin-sericite altered East porphyry (white); D3848 \pm 38 m. E. Veinlet of anhydrite with red amorphous hematite and minor coarse-grained covellite-digenite (opaque); D2743-282.8 m. Transmitted light, crossed polars. F. Sphalerite rim on chalcocopyrite grain replaced with coarse-grained covellite-(digenite); coarse-grained covellite and/or digenite form inner rims inside almost all sphalerite rims. D2743-53.7 m. G. Segmented 2-m blue quartz-molybdenite vein (outlined, arrow, left) and rare late N 70° E fault (arrow, right) cutting megabreccia zone; M3 bench, ± 4500 N-3800E. H. Segmented pyrite-enargite veins (arrows) in 50- to 100-m-wide fault breccia zone next to the West fault; no quartz vein clasts or continuous veins of any type in this zone; top of photo is to left; M3 bench near G.



alteration, but this is due to superposition of younger pyritic veins following the same structures. Veins and veinlets of the main-stage contain pyrite, chalcopyrite, bornite, and digenite, decreasing amounts of quartz and increasingly well developed sericitic alteration halos (Fig. 4D). Locally, the earliest of these veins appear to contain pyrite without Cu sulfide (Fig. 4C; Lindsay et al., 1995). Relatively late main-stage veins contain enargite \pm pyrite and minor sphalerite. Later still, veinlets and fractures are filled with relatively coarse grained covellite (to 1 mm) and digenite with and without pyrite. Lindsay et al. (1995) have drawn the analogy of this sequence with the evolutionary sequence of A, B, and D veins described at El Salvador (Gustafson and Hunt, 1975). Whereas, in a gross sense of changing chemical environments the analogy has some validity, Chuquicamata has a much more complicated history and a modified nomenclature is required here.

The gross pattern of fault veins (veins following faults and with subsequent faulting) compiled to a 1:2000 scale (Fig. 5A) has been presented and discussed by Lindsay et al. (1995), Rojas and Lindsay (1997), and Lindsay (1998). Only the most continuous veins, those traceable for three benches or more (i.e., >39 m), are shown in Figure 5A. Lack of continuity of veins and faults is due to the abundance and complexity of crosscutting and offsetting faulting. Most faults have moved prior to, during, and after whatever mineralization is in them, and most veins have more than one stage of superimposed mineralization. In general, early north-south to northeast-striking fault veins show pre- to synmineral, dextral movement, with superimposed sinistral reactivation, and contain all stages of mineralization. Northwest-striking structures are younger, show sinistral movement, and are largely barren, except for minor enargite-sphalerite and covellite-digenite mineralization. Also shown in Figure 5A is the approximate outline of quartz stockwork. Although poorly defined by present mapping, the outline encloses the more abundant (roughly >1 vol %) small-scale quartz veins and veinlets. These include all quartz veins, both randomly oriented and in parallel sets, without regard to stage of mineralization or orientation.

Faults and fault breccias

All of the structures on both sides of the West fault shown in Figure 2 are faults with postmineral movement (i.e., following the last mineralization), although mineralization is present only very locally to the west. Those shown as fault veins are faults following veins, which themselves occupy earlier faults. Compared to Figure 5A, Figure 2 extends above the top of relatively frequent mapping (H-1 bench) and has been simplified to show only the largest structures. Only the north-south-trending set of West fault structures itself, portions of the Americana fault system, which is parallel to it at the east edge of the brecciated quartz-sericite zone in the south part of the pit, and most of the northwest-trending faults do not follow previous veins. They show entirely post-mineralization, sinistral displacements (Tomlinson and Blanco, 1997). In that some of the northwest structures contain enargite-sphalerite \pm pyrite veins, and also minor coarse-grained covellite-digenite without pyrite, this structure set appears to have been formed late during main-stage mineralization (Lindsay et al., 1995; F. Ramírez, pers. commun., 1994). A 35 \pm 1-km net offset has been demonstrated for the West fault

system (Dilles et al., 1997; Tomlinson and Blanco, 1997), much of it concentrated on the 1- to 5-m-thick gouge of the main strand of the West fault and the \pm 400-m-wide zone of braided shears with montmorillonitic gouge within the Fortuna Intrusive Complex (Lindsay, 1998). It is not clear when movement began on this structure, but clasts of supergene chalcocite showing slickensides indicate movement younger than 19 to 15 Ma, the age of supergene alunite (Sillitoe and McKee, 1996). Within the brecciated quartz-sericite zone there are multiple parallel discontinuities, some with discontinuous gouge and some with no gouge, which probably are faults that also have had important displacements associated with displacement on the West fault. Among these are the discontinuities at the western edge of the quartz-molybdenite veins and the eastern edge of disseminated enargite with no other veins (Fig. 5B; see below). The breccia zone itself, and indeed most of the quartz-sericite zone, has experienced very intense, largely postmineral fault brecciation. Rotated clasts of quartz-molybdenite veins up to 2 m thick but less than 5 m long are common (Fig. 4G), and even late pyrite-enargite veins are fragmented (Fig. 4H) in what has been named "megabreccia" (breccia symbol, Fig. 2). Particularly in the western margin of this zone, within about 30 m of the central West fault gouge, almost no clasts larger than 5 cm are present. Very few faults and fewer veins cut this breccia, but rare minor faults offset even the West fault gouge.

Hypogene Alteration and Mineralization

The gross patterns of alteration and sulfide mineralization within the orebody, as exposed in the pit at the end of 1995, are shown in Figure 5A and B and in cross section in Figure 6A and B. Below are described details of these patterns and their time and genetic relationships. Because of extensive superposition of pyrite as part of main-stage sulfide assemblages, pyrite is present everywhere on this scale even though not listed in the key. The sulfide section (Fig. 6B), however, is not directly comparable to the plan (Fig. 5B) as it is derived from different data sets. The plan is the result of pit mapping of dominant sulfides compiled to a 1:2000 scale, while the section is the pattern of sulfide-alteration ore types from the computerized ore reserve model. Although As is normally carried in a separate model, the zone where enargite is the dominant copper sulfide mineral has been added to Figure 6B. After 83 yr of pit operation, practically all of the leached capping and most oxide ore have been removed. Although supergene chalcocite and covellite are still present in much of the pit, primary sulfides comprise an increasing proportion of remaining. Strong supergene enrichment remains primarily in the deep trough with intense sericitic alteration within the central and southern parts of the pit. As discussed below, the deep trough of chalcocite and covellite (Fig. 6B) is largely supergene but there is also abundant hypogene chalcocite (including djurleite and digenite) and covellite at depth, and it has not been possible to clearly define the base of supergene enrichment. As at El Salvador and many other porphyry copper deposits, vein relationships lead to the definition of an early stage defined by K feldspar stable alteration and early quartz veinlets, a transitional stage defined by quartz-molybdenite veining, and a main-stage defined by pyrite-bearing

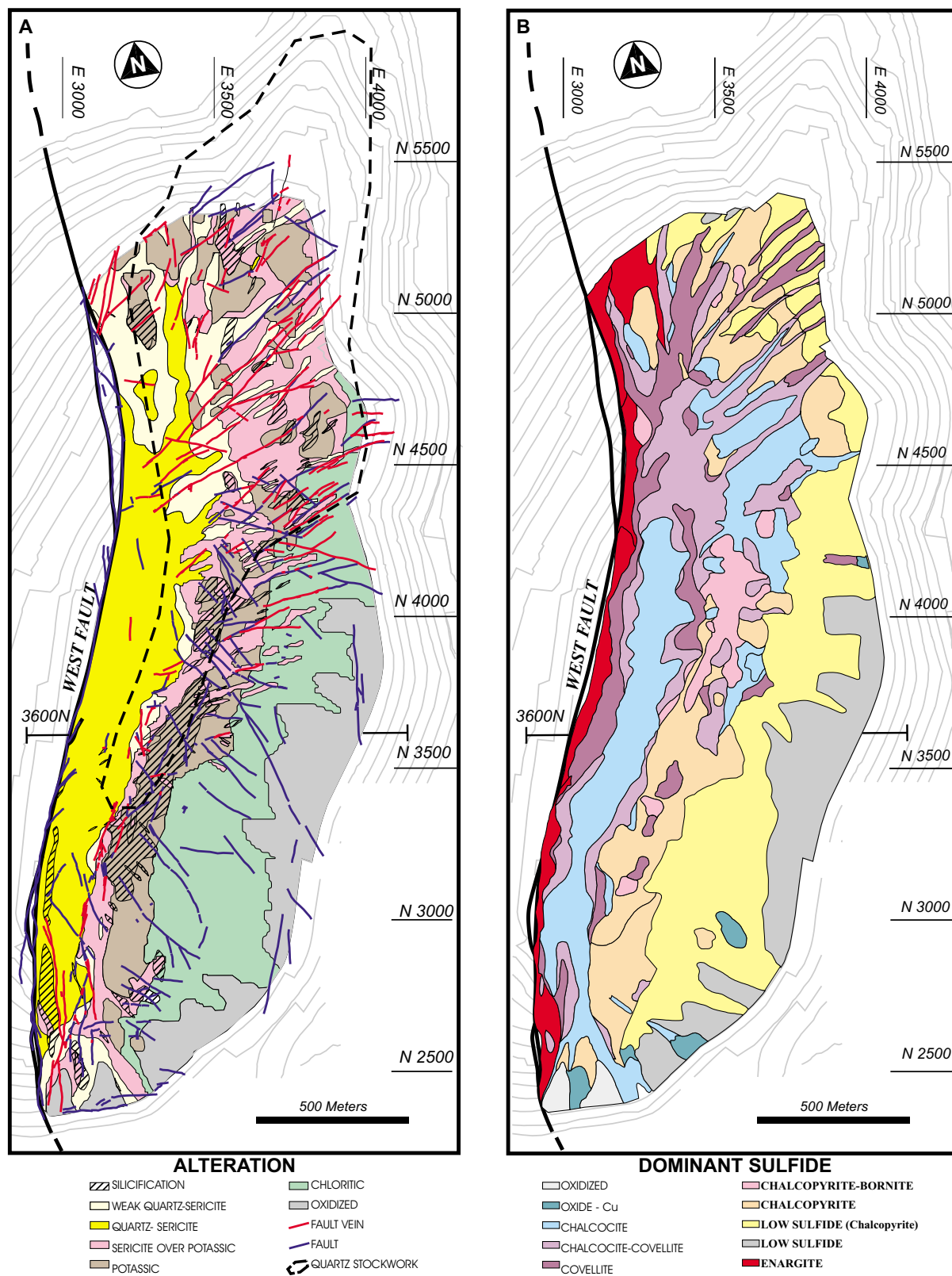


FIG. 5. A. Dominant alteration type and major structures exposed in open pit as of 1995, in area of orebody; from 1:2000 mapping by Rojas and Lindsay (1997). Oxidized rock lies above the top of sulfide but is not necessarily leached. Megascopic silicification is partly equivalent to quartz-K feldspar alteration. See text for discussion of approximate outline of quartz stockwork. B. Dominant copper sulfide exposed in open pit as of 1995; pyrite is ubiquitous, mostly associated with main-stage veins, which are most abundant in quartz-sericite and sericite over potassic alteration zones. Bottom bench is 2,437 m, top mapped bench is 2,697 m (pit surface slightly above that in Fig. 2).

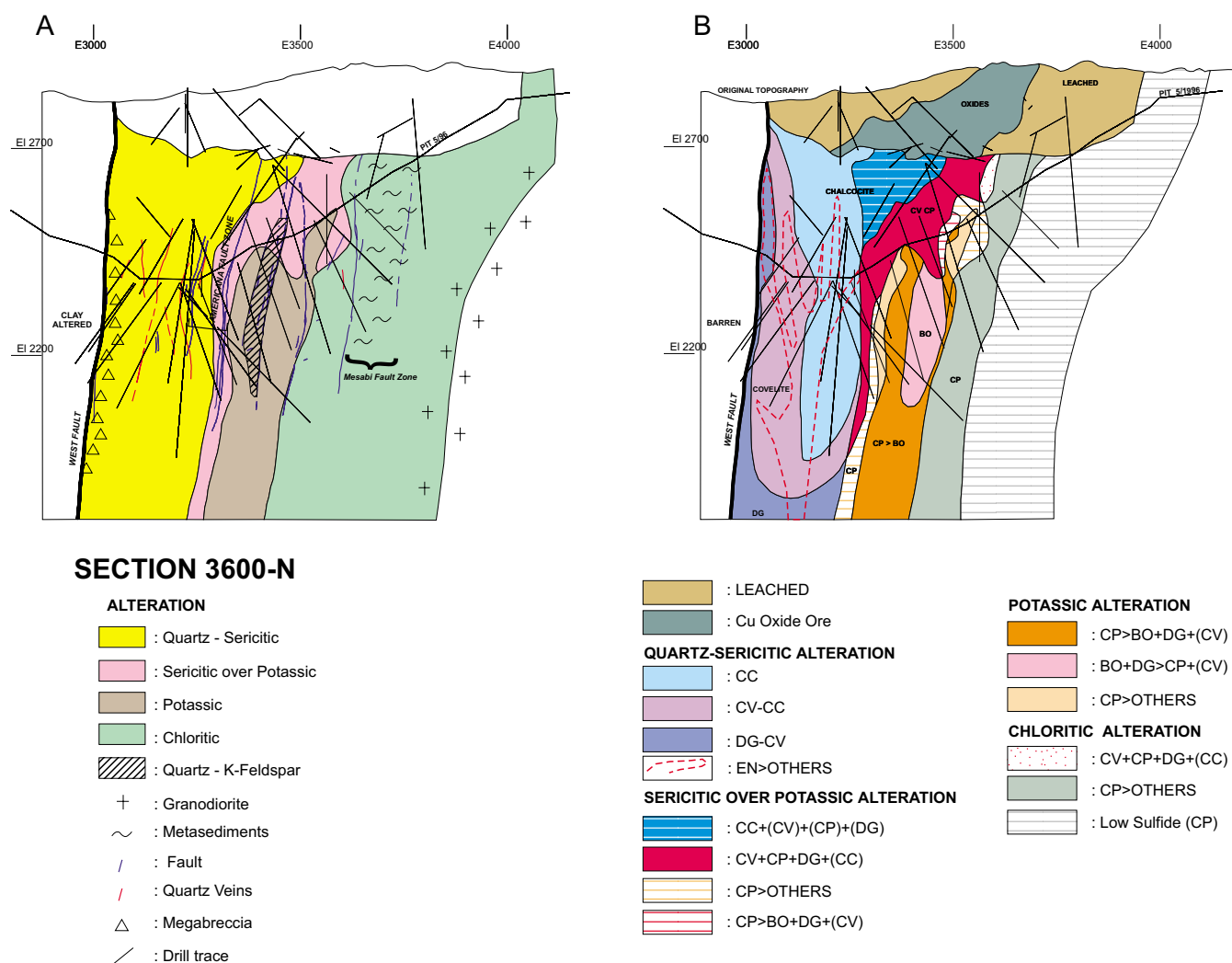


FIG. 6. A. Dominant alteration type and major structure in 3600N section; computerized geologic model of May, 1996; trace of diamond drill holes shown. Old data on alteration assemblages above the top of sulfide (blank area) have not been carried forward in the model. B. Dominant copper sulfide alteration associations in 3600N section; modified geologic model of September 1995; pyrite is ubiquitous, associated with main-stage veins but is absent in the bornite-bearing background assemblages shown.

veins with sericitic halos. A more unusual and controversial late stage is defined by coarse-grained covellite-digenite veinlets without pyrite and possibly hypogene sphalerite rims on other sulfides (Fréaut, et al., 1997).

Early-stage alteration and mineralization

The earliest events decipherable after consolidation of the porphyries are formation of potassic alteration and more local quartz and K feldspar-quartz veinlets. Secondary biotite occurring as veinlets and replacing hornblende phenocrysts is characteristic of the potassic zone, whereas quartz veinlets and secondary K feldspar, occurring as veinlets and replacement of plagioclase throughout the rock and as halos on the early veins, are more restricted. Unfortunately, mapping has not been detailed enough to define the distribution of these early-stage quartz veinlets. Anhydrite, variably hydrated to gypsum and leached from much of the orebody by supergene solutions, is a component of potassic alteration assemblages

and of all other subsequent stages of hypogene alteration and mineralization. Early quartz veinlets in the quartz-sericite zone indicate that potassic alteration originally extended into this zone as well. At the north end of the pit, potassic alteration widens westward around the end of the sericitic zone, and a northward-widening wedge of chloritic alteration separates it from the West fault beyond the edge of mapping in Figure 5A. In a few deep drill holes below the south part of the pit, residual potassic alteration extends westward up to the West fault. Figure 3B shows a quartz-K feldspar vein clearly crosscutting weak foliation in West porphyry and which shows variable granular texture apparently affected by recrystallization and shearing parallel to the vein walls. The vein has both a K feldspar alteration halo and minor disseminated molybdenite-chalcocopyrite, compared to sparse disseminated chalcocopyrite-bornite in the K feldspar-biotite altered porphyry. More typically, early-stage quartz and quartz-K feldspar veins carry practically no sulfide. Although described

above as probably magmatic features, K feldspar megacrysts can also be argued to be potassic alteration features. Their distribution is independent of other textural variation in East, West, and Banco porphyries and appears to be related to the pattern of Banco porphyry. The presence of replaced or resorbed inclusions of plagioclase in some megacrysts also supports this interpretation. All of the rocks within the Chuqui Porphyry Complex are affected by potassic alteration and are cut by at least some early-stage veins. Plagioclase in potassic-altered East porphyry is completely changed to albite, whereas in Banco porphyry residual magmatic plagioclase can be found (A. Arnott, pers. commun., 2000). All of the porphyries have been subjected to pervasive cataclastic deformation (see Fig. 3A-C, E-G). Quartz is prone to recrystallization to polycrystalline aggregates, and elongated polycrystalline quartz phenocrysts are seen in rock with scant megascopic evidence of deformation. Biotite phenocrysts are commonly bent in rock with cataclastic fragmentation and kinking of plagioclase phenocrysts, but K feldspar crystals are broken only in very strong cataclastically deformed rock. This deformation is pervasive with variable intensity throughout the entire ore-body but is most strongly developed in the quartz-K feldspar alteration zone and in smaller and apparently discontinuous mylonite zones.

Quartz-K feldspar alteration is interpreted as a distinct alteration type. It occurs in a band of hard white to gray rock with obliterated texture, trending N 20° E across the potassic zone, from about 3000 to 4700 N (silicification, Fig. 5A). In cross section this band occurs as a steeply west-dipping zone up to 200 m wide. Quartz-K feldspar differs from normal potassic alteration in that biotite is completely replaced by K feldspar and quartz, the texture is further obliterated by pervasive cataclastic deformation and streaking with fine-granular quartz-K feldspar (Fig. 3E, F, and G), and added silica occurs as a fine granular replacement with K feldspar rather than as quartz veinlets. Within the zone, quartz-K feldspar alteration is irregularly developed in streaky bands with residual potassic alteration containing more or less unmodified rock texture and biotite. Only East porphyry occurs in the quartz-K feldspar zone, but this appears to be the southward extension of the cluster of discontinuous Banco porphyry dikes (Fig. 5A vs. Fig. 2). Any residual plagioclase in the rock is albite. Cataclastic deformation of fine twinning in this secondary albite (Fig. 3E) indicates that albitization preceded quartz-K feldspar alteration. K feldspar megacrysts are not replaced by this albitization, which may be related to earlier potassic alteration, but are locally veined by K feldspar (Fig. 3F). Most early quartz veins and even many quartz-molybdenite veins throughout the broad zone of weaker pervasive alteration are thoroughly recrystallized to a fine-granular equilibrium texture, with 120° intersections of grain boundaries and loss of most fluid inclusions. In most of the quartz-K feldspar band there are no quartz veins, so the timing of this deformation relative to vein evolution is uncertain.

A second, less well defined zone of silicification and lacking original biotite trends north-northeast between 3500 and 3600E at the north end of the pit (J. P. Hunt, unpub. report, 1962). This zone has much less intense cataclastic deformation and texture obliteration than the main quartz-K feldspar zone, but within it at least some quartz-molybdenite veins are

segmented and intensely recrystallized. It is not entirely clear whether this deformation of the veins is related to quartz-K feldspar alteration, indicating that quartz-K feldspar alteration is a separate and later stage of alteration from normal potassic alteration. Alternatively, quartz-K feldspar could be simply an extreme and continuous development of potassic alteration.

The dominant background sulfide association in the potassic zone is chalcopyrite-bornite without pyrite, although in most of the zone bornite is subordinate to chalcopyrite (the chalcopyrite zone in Fig. 5B shows dominant sulfide only). The quartz-K feldspar zone corresponds generally with the zone of bornite-digenite-chalcopyrite, the apparent center of early-stage sulfide zonation. However, coarse-grained covellite commonly accompanies the digenite and most sulfides are in fractures and brecciated zones (Fig. 3H). The abundance of sulfide, and therefore Cu grade, is highly dependent on brittle fracturing that appears to be superimposed, possibly much later, on the cataclastic quartz-K feldspar environment. Pyrite is absent outside of main-stage veins and sericitic halos, but there is widespread local development of green sericite in highest grade quartz-K feldspar zones, which contain abundant digenite and coarse-grained covellite. The abundance of high-grade zones within the quartz-K feldspar zone diminishes downward, and laterally quartz-K feldspar without superimposed fractures contains only sparse chalcopyrite-bornite mineralization.

Propylitic assemblages with chlorite and epidote and specular hematite veinlets are clearly superimposed on the eastern edge of the potassic alteration zone, where there was only alteration of hornblende to biotite but no quartz veining or destruction of magnetite. Anhydrite and minor K feldspar and biotite occur occasionally in specularite veinlets that cut biotite-magnetite-chalcopyrite veinlets and are cut by chalcopyrite-pyrite veinlets. Pervasive deformation declines markedly in this zone. Propylitic alteration clearly predates alteration halos around main-stage veins, but an absence of quartz-molybdenite veins in this outer zone precludes determination of its timing relative to this veining. By analogy with other porphyry copper deposits (e.g., Gustafson and Hunt, 1975), chloritic alteration along with the low-intensity chalcopyrite-pyrite mineralization of the outer zone is considered part of the early stage. Eastward within the chloritic (= propylitic) alteration zone (Fig. 5A) the abundance of sulfide decreases to less than 0.5 vol percent (low sulfide, Fig. 5B), but pyrite is still subordinate and there is no pyritic halo similar to many other deposits.

Quartz-molybdenite stage

Molybdenite is conspicuous at Chuquicamata, almost all of it carried by quartz veins as disseminated crystals and as "smears" in cracks. A phase of generally <1-cm veins with relatively little molybdenite cuts early-stage quartz and quartz-K feldspar veins. K feldspar is usually not present in molybdenite-bearing veins, but Figure 3B shows a vein apparently transitional in characteristics and perhaps also in time. Large (blue) quartz veins with abundant molybdenite cut these older veins (Waterman, unpub. report, 1951; Lindsay et al., 1995). The later large veins are typically 0.5 to 1 m or more in width and are commonly banded. Figure 4A and B illustrate

textures found in a blue vein from the northeast part of the pit where there has been relatively little overprinting by subsequent events. Some of the banding is due to shear recrystallization, parallel to the walls, of originally coarse-grained quartz (up to 1.5 cm) tending to be elongate perpendicular to the walls. Some of the banding is due to concentration of residual coarse-grained molybdenite on stylolites. Main-stage veins, characterized by pyritic assemblages and sericitic alteration, clearly cut quartz-molybdenite veins. Reopening of earlier formed veins and overprinting of younger sulfide and alteration halo assemblages are ubiquitous, to the point that it is a very rare vein which represents only a single stage of mineralization. This is why most quartz-molybdenite veins appear to have sericitic halos, but the rare occurrences demonstrate that at least the smaller veins and probably the blue veins were not formed with sericitic halos.

There is a strong correlation between the abundance of quartz veins and Mo grade. Figures 7B and 8B illustrate the distribution of Mo exposed in the pit and on the 3600N section (see also Quinteros and Fréaut, 1997). Very high values, 0.07 to 0.25 percent Mo, are concentrated in the quartz-sericite alteration zone, widening northward and splaying off to the northeast between about 4100 and 5000N. Particularly in the western portions of the orebody, quartz-molybdenite veins have been severely dislocated by faulting and brecciation (Fig. 4G). The pattern is asymmetrical, with an abrupt western edge of moderate Mo values (>0.01%) and quartz veins, and a more gradational decline of quartz veins and Mo values to the east. In several sections, this western edge is as much as 100 m east of the mapped West fault, representing a subtle fault. An upward and eastward spread of moderate Mo values (more evident in sections other than 3600N) seems to represent the distribution of "smear moly" in wall rock more than an increase in quartz veins. Here, as in other porphyry deposits, this smear moly appears to have been remobilized by subsequent hydrothermal activity as well as locally by simple mechanical movement.

Main stage

Pyritic veins and quartz-sericite alteration of the main stage of mineralization obliterate almost all traces of earlier assemblages in the western side of the orebody adjacent to the West fault (Figs. 6 and 7). Copper emplaced during the main stage, plus supergene enrichment of largely main-stage assemblages, accounts for most of the metal production to date and a large proportion of future reserves, although this proportion is impossible to quantify. Sulfide veins of this stage are defined by sericitic alteration halos and assemblages of pyrite with varying proportions of quartz, Cu-Fe sulfides, enargite, tennantite, and sphalerite (Fig. 4C and D). These veins invariably cut quartz-molybdenite veins but locally contain minor smear molybdenite. In practically all respects they are analogous to main-stage veins at Butte (Meyer et al., 1968), Rosario-Poderoso veins at Collahuasi (Hunt, 1985), and "D" veins at El Salvador (Gustafson and Hunt, 1975). The quartz-sericite zone represents merging of sericitic halos of this stage of mineralization, and only in the weak quartz-sericite areas (Fig. 5A) can original rock texture be discerned. Upward and eastward, the zones of quartz-sericite and sericitic over potassic alteration encroach on the potassic zone, accompanying pyrite with chalcocite and covellite (Fig. 6A). Within this

upper zone, K feldspar is more resistant than plagioclase and biotite to alteration to sericite but is commonly altered to supergene kaolinite. Only to the east and north of the quartz-sericite zone can earlier assemblages be seen between main-stage veins, but even here there is a more or less pervasive overprinting of main-stage assemblages in largely discontinuous fine-scale shatter veinlets and dissemination. Only where veins or veinlets of a single substage have escaped reopening but are crosscut by later substages can unambiguous definition of main-stage vein evolution be constructed. Only a preliminary description can be given here. Lindsay (1998) provides a discussion of the various vein sets mapped in the pit.

Principal vein assemblages are pyrite-chalcopyrite-bornite, pyrite-bornite-digenite \pm enargite, and pyrite-digenite-covellite \pm enargite. Quartz is abundant in the earlier formed main-stage veins, but it is commonly difficult to be sure the quartz is not inherited from an earlier quartz-molybdenite vein with only minor molybdenite. Pyrite is the only sulfide in some veinlets (Fig. 4C) and is very abundant (pyrite >3.5% by vol based on Fe assays) in the high enargite part of the quartz-sericite zone. Enargite-pyrite in veins is dominant within much of the quartz-sericite zone and also as disseminated sulfides along a narrow brecciated band next to the West fault. The outline in Figure 6B of enargite greater than other copper minerals is derived by calculation of As vs. Cu assays. The sequence of assemblages appears to be pyrite-chalcopyrite-bornite \rightarrow pyrite-bornite-digenite \rightarrow pyrite-digenite-covellite, from early to late and upward in the deposit. Enargite appears to join the assemblage relatively late but was abundant in veins mined in the uppermost elevations in the northeast part of the orebody, which were apparently related to the early-formed northeast-trending fault system (F. Ramírez and W. Chavez, unpub. report, 1997; Lindsay, 1998). These veins are almost unrecognizable in the present pit and have apparently zoned downward into pyrite to the point that there is practically no As left. Chalcocite, digenite, and covellite, along with pyrite and enargite, are the dominant sulfides in the western part of the orebody (Figs. 5B and 6B). Digenite is largely hypogene. Chalcocite is clearly supergene at higher elevations, commonly sooty, occurring as thick rims on pyrite and other sulfides and extending to greatest depth where the alteration is least reactive. Fine-grained covellite increases relative to chalcocite downward within the flat west-dipping enrichment blanket and extends an undefined distance down the western trough of chalcocite. It rims chalcopyrite and other primary sulfides and is of supergene origin. At depth, however, relatively coarse grained covellite, typically 0.5 to 2 mm and occurring with digenite and locally anhydrite showing no hydration to gypsum, is clearly hypogene (e.g., Lewis, 1996). Also, chalcocite may be intergrown with coarse-grained covellite or bornite and may lack rimming textures suggestive of supergene origin. It is very difficult to distinguish supergene from hypogene chalcocite and covellite even with the aid of a microscope. Because of this the lower limit of supergene enrichment is not shown in Figure 6B. One measure of the intensity of enrichment is the degree of replacement of enargite, the mineral after pyrite most resistant to replacement. The upward fingering out of enargite greater than other Cu minerals in Figure 6B is due to this replacement but shows abundant residual enargite in much of the chalcocite trough.

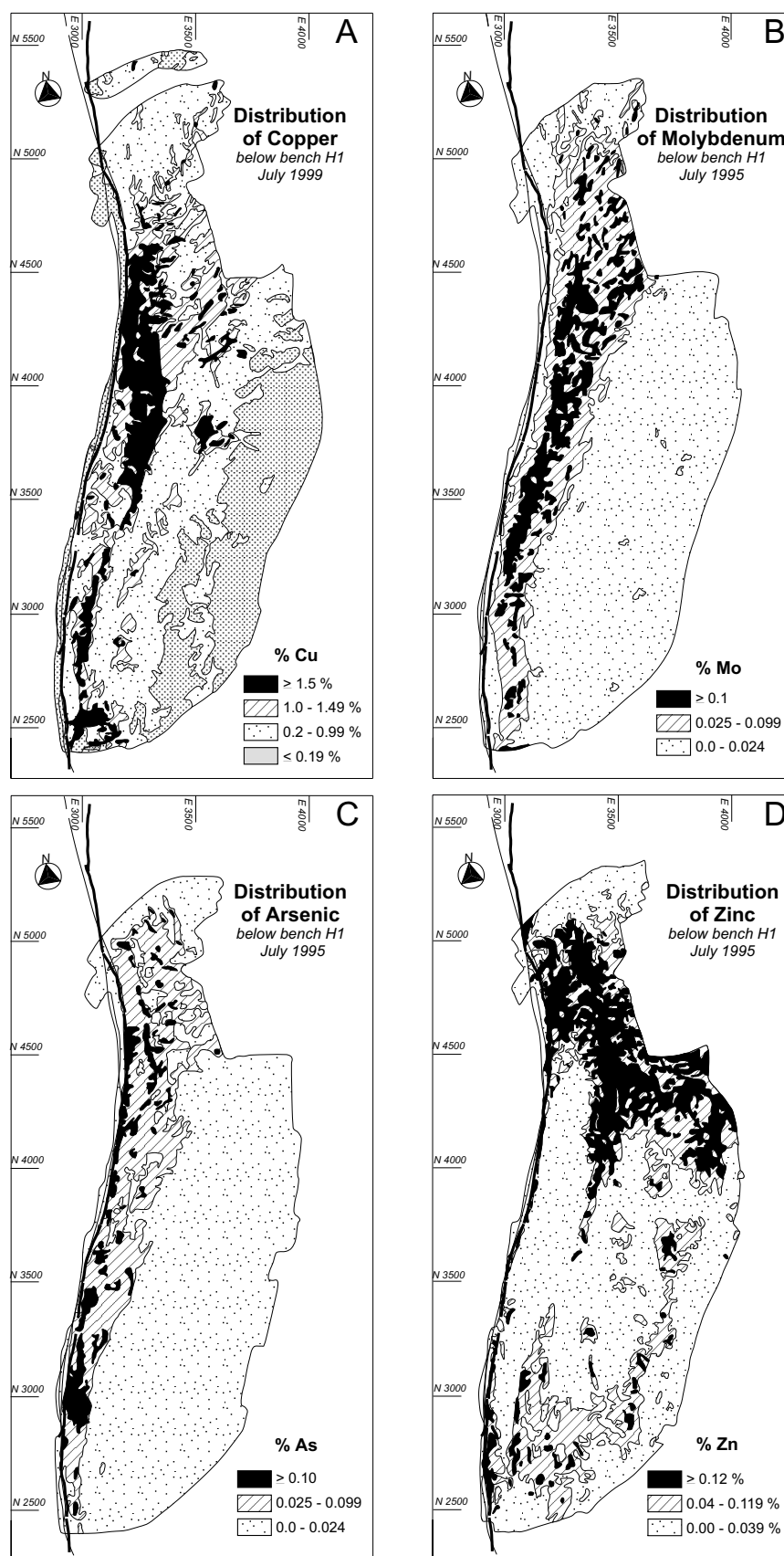


FIG. 7. A-D. Distribution of copper, molybdenum, arsenic, and zinc in the open pit below bench H1 (2,697-m elev), from blast hole assays. A. Data from July 1999. B, C, and D. Data from 1995 (same surface as Fig. 5A and B).

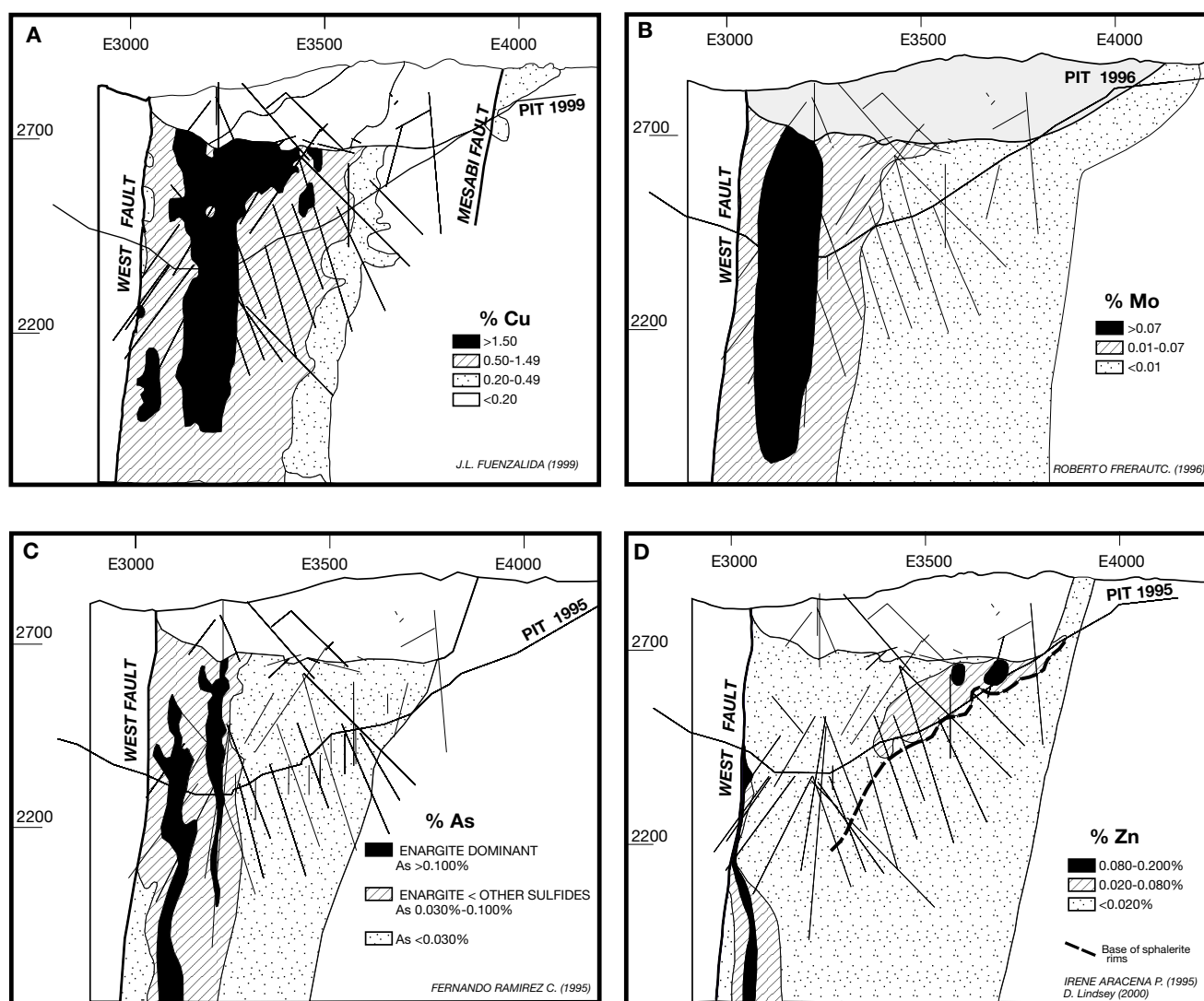


FIG. 8. A-D. Distribution of copper, molybdenum, arsenic, and zinc in 3600N section, from diamond drill hole and blast holes.

Although sericite-quartz is the alteration typically associated with main-stage veins, alunite also occurs locally with pyrite-enargite mineralization. The alunite has widely varying texture, including coarse-grained, high-birefringent flakes and coarse-grained pseudocubes with occasionally intergrown phosphate minerals typical of hydrothermal origin (Stoffgren and Alpers, 1987). There is a gradation in grain size of alunite down to very fine grained salt and pepper alunite, which occurs commonly with kaolinitic clays and supergene chalcocite. As in the case of covellite, it is commonly difficult to distinguish hypogene from supergene alunite at Chuquicamata. One would expect to find pyrophyllite and/or dickite occurring with alunite in high-sulfidation assemblages of pyrite, enargite, covellite, and digenite. Only traces of pyrophyllite and dickite have been detected locally, even though hundreds of sericite samples have been X-rayed. However, too little work has been done to be sure that locally more typical advanced argillic alteration has not been developed, particularly at higher elevations.

Sphalerite (with 0–5 wt % Fe; M. Zentilli and M. Graves, unpub. report, 1993) is common in many veins with enargite, including veinlets which contain little or no pyrite but may contain covellite-digenite. These latter veinlets occupy late-formed northwest structures. Minor tennantite occurs with pyrite-chalcocopyrite in veins and veinlets within the potassic zone and contains up to 8 wt percent Zn (M. Zentilli and M. Graves, unpub. report, 1993).

The only fluid inclusion study to date is reported in the undergraduate thesis of M. Vega (1991), who found fluids ranging from 250° to 350°C and 2 to 20 percent NaCl equiv in quartz from a variety of quartz-molybdenite and main-stage veins. Whereas these are plausible main-stage fluids, it is unlikely that they represent fluids that formed the now strongly recrystallized quartz-molybdenite veins.

Late stage

Covellite in the main-stage veins is relatively coarse grained (to 2 mm), contains 0 to 4 wt percent Fe (M. Zentilli, unpub.

report, 1996; Lewis, 1996), extends to more than 600 m below the present pit bottom, and locally occurs with anhydrite. It is clearly of hypogene origin, although at upper elevations it is commonly difficult to distinguish from supergene covellite. Its abundance is shown by the extent of covellite-dominant assemblages shown in Figures 5B and 6B. A substantial but poorly documented proportion of this covellite is intimately associated with digenite, occurring in cracks and veinlets without quartz, pyrite, or other sulfides. It appears to constitute a distinct late stage. Many of these late veinlets contain red hematite and locally also anhydrite (Fig. 4E; Quinteros, 1997). The eastward flare of covellite shown in Figure 6B may be more due to this primary covellite than to covellite formed as the lower zone of incipient supergene enrichment. Covellite extends downward in the high bornite zone and with digenite represents a significant proportion of copper in the orebody. Because earlier formed pyrite is so widespread, it is very difficult to see where covellite-digenite-pyrite of the main-stage terminates, and where that of the late stage without pyrite begins; indeed they probably constitute a continuous evolution.

A striking feature which largely coincides with the eastward-flaring covellite zone is a zone of moderate to high Zn values (0.02 to >0.08 wt % Zn; Figs. 7D and 8D), largely due to rims of sphalerite on chalcopryite and other copper sulfides (Fig. 4F; Aracena et al., 1997). Another zone of moderate to high Zn values extends to depth along with high As (Fig. 8D and C) and correlates with the presence of coarse-grained sphalerite in the enargite veins. Low Zn values below the Zn zone in the east are contained in traces of sphalerite and Zn-bearing tennantite within pyrite-bearing veinlets. There is a sharp top of Zn values at the base of the west-dipping chalcocite enrichment blanket and extending around the deep trough of chalcocite. Sphalerite rims are continuous in a band roughly 100 to 200 m wide below this top of Zn and extending from the anomalous Zn zone in potassic and chloritic alteration in the east (Fig. 8D) across the quartz-sericite zone in the west. This distribution and their textures are suggestive of their being formed as a lower zone to the supergene chalcocite blanket (Aracena et al., 1997). However, Figure 4F also illustrates the occurrence of inner rims of coarse-grained covellite and/or digenite with the sphalerite rims. This photograph shows the coarse grain size of the covellite but does not illustrate as well the near continuous inner rim of digenite-covellite under sphalerite, which is ubiquitous and so abundant that it strongly suggests the sphalerite rims are coeval with the late-stage covellite-digenite veining without pyrite. We have yet to find sphalerite rims occurring within anhydrite-saturated rock, which would confirm their hydrothermal origin. Iron content of rim sphalerite is 0 to 1.2 wt percent, highest where rims are on chalcopryite.

Supergene Mineralization and Alteration

The rich oxide copper orebody described by Taylor (1935) and Jarrell (1944) has been largely mined out, but substantial resources of lower grade material remain in the north end of the pit and beyond (North zone, Fig. 1; Cuadra et al., 1997; Ossandón and Zentilli, 1997). Oxide ores contain a large variety of minerals but primarily antlerite, brochantite, atacamite, chrysocolla, and copper pitch. Wall-rock alteration mineralogy of the oxide ores is not well documented but was mostly

quartz-sericite with increasing kaolinitic clay and residual K feldspar to the east and at depth. Copper oxide ore contains residuals of chalcocite and was overlain by leached capping. Figure 6B shows that the oxides were an eastward and upward extension of the chalcocite zone, indicating it was a supergene chalcocite enrichment blanket oxidized in situ. More obvious in other sections to the north (Taylor, 1935), this is the upper of two chalcocite blankets with a leached horizon in between. A lower enrichment zone is less well developed in lower grade protore and more reactive alteration assemblages and contains decreasing chalcocite and/or covellite proportions downward. However, in the central zone of intense brecciation, which contains nonreactive quartz-sericite alteration and very pyritic veins, the two enrichment blankets merge as both copper leaching and chalcocite enrichment reach maximum depths.

This is the largest supergene enriched orebody in the world and clearly a large thickness of leached capping above the premine surface was required to produce the copper. Little remains either as written description or core from the leached capping removed by mining. In the north, the leached rock both above and below copper oxide is largely goethite with earthy jarosite, what one would expect from oxidation of moderately pyritic protore (Anderson, 1982). Within the copper oxide horizon, there are more Fe-rich, steep structural zones within which copper has been leached. The limonite here is hematitic, as one would expect from oxidation of chalcocite-enriched pyritic vein zones, and again consistent with the interpretation of two stages of oxidation and sulfide enrichment related to a changing water table.

Anhydrite, variably hydrated to gypsum, is a component of each of the hypogene alteration assemblages and completely saturates all porosity in rocks in which it occurs. It had to be leached by supergene solutions before any supergene leaching or enrichment of sulfide could occur. Only in some deepest drill holes, more than 800 m below the premining surface, continuous intervals of this sulfate zone rock, similar to rock in the sulfate zone of many porphyry copper deposits, are encountered (Hunt, 1969; Gustafson and Hunt, 1975). As deep as 1,200 m below the premine surface, anhydrite has been hydrated and leached from most fault zones, and what was once a continuous sulfate zone has been reduced to isolated residuals of gypsum and rarer anhydrite diminishing upward between structural zones.

Very important quantities of copper were leached from the oxidized capping and probably from the chalcocite blanket and moved laterally. Originally over 300 Mt of exotic copper ore was deposited in gravels south of the pit to constitute the Exótica orebody (Fig. 1; Table 1). This orebody contained flat high-grade veins of chrysocolla and copper pitch, within variably altered gravels cemented by chrysocolla, with minor atacamite, copper wad, and pitch (J. P. Hunt, unpub. reports, 1963 and 1965; Newberg, 1967; Mortimer et al., 1977; Munchmeyer, 1996). Exotic copper in gravels extends from the upper south benches of the Chuqui pit, through the South mine to at least 7 km south, and there are important occurrences north as well (Fam and Rojas, 1997).

Geochronology

There have been many published attempts at dating events at Chuquicamata by Makshev and Zentilli (1988), Makshev et

al. (1988), Sillitoe (1988), Boric et al. (1990), Maksaev (1990), Zentilli et al. (1995), Sillitoe and McKee (1996), and Reynolds et al. (1998). And there are numerous dates that have not yet been presented for publication, particularly by M. Zentilli at Dalhousie University with L. Heaman at the University of Alberta, J. Ballard and coworkers at the Research School of Earth Sciences of Australian National University, and by J. Ruiz and coworkers at the University of Arizona. The dating of significant events at Chuquicamata has proven to be an extraordinarily difficult problem, and it is impossible to attempt a detailed analysis here of the many conflicting dates. Definitive conclusions may only be reached after full presentation of the data, but we cannot avoid trying to make some sense of results to date. The following ages, done with the latest technology, appear to us to be the most reasonable.

An age of 31.1 ± 0.2 Ma is consistently indicated by $^{40}\text{Ar}/^{39}\text{Ar}$ dating of sericite formed during the main stage of mineralization. Discerning events prior to this time, through the intense mechanical deformation and thermal overprint of this stage, have been much more difficult. Biotite and feldspar in the potassic alteration zones relatively distant from major sericitic veins and at higher elevations yield $^{40}\text{Ar}/^{39}\text{Ar}$ ages of 35 to 34 Ma, whereas closer to zones of sericite alteration and from deep below the pit they yield ages of 31 to 32 Ma (Reynolds et al., 1998). Joaquín Ruiz (writ. commun., 1998) has obtained an age of molybdenite of 34.9 ± 0.17 Ma, collected from a typical blue quartz vein using the Re-Os technique. Larry Heaman and Marcos Zentilli have obtained several U-Pb single grain and multigrain ages in zircon from East porphyry. These suggest zircon crystallization at 35 to 36 Ma and the presence of inherited grains with 37 to 38 Ma ages. Julian Ballard (writ. commun., 2000) has applied eximer laser ablation inductively coupled plasma mass spectrometry (ELA-ICP-MS) dating of zircon from the intrusive units; preliminary ages are 34.8 ± 0.3 Ma for East porphyry, 33.3 ± 0.3 Ma for West porphyry, and 33.4 ± 0.4 Ma for Banco porphyry. Apatite fission track dating and track length modeling for the region indicate that probably 4 to 5 km of rock were eroded during the exhumation of the Chuquicamata block between 50 and 30 Ma (Maksaev, 1990; Maksaev and Zentilli, 1999), a time period that immediately precedes and overlaps the emplacement and mineralization of the Chuqui Porphyry Complex. Fission track dates in apatite within the deposit yield ages of 30 Ma (Maksaev, 1990), indicating fast cooling of the system to ca. 100°C soon after the main stage of mineralization. K-Ar dating of alunite by Sillitoe and McKee (1996) estimates the age of supergene enrichment and alteration at 15 to 19 Ma.

At present, based on the dating and consistency with geologic reasoning, we can conclude that East porphyry is probably significantly older than West and Banco porphyries, and that all were emplaced before 33 Ma. Potassic alteration and subsequent quartz-molybdenite veining was probably closely associated with the emplacement and cooling of West, Fine Texture, and/or Banco porphyries. Main-stage hydrothermal activity followed at least 2 m.y. later as a separate event, but intrusion related to this event has not been identified. To elucidate just how long it took to emplace the intrusive rocks, and to evolve early and transitional stages of mineralization will require more work. Also, it remains to be determined where

quartz-K feldspar alteration fits in and whether some of the pyrite- and sericite-forming hydrothermal veins were related to the cooling of the porphyries and distinctly older than the main stage. The dating program is still in progress and will be reported in more detail in subsequent publications.

Discussion

Evolution of mineralization

Premain stages: There is a clear succession of intrusion of East porphyry → Banco porphyry, followed by potassic alteration (biotite formed and texture largely preserved), and early-stage quartz-K feldspar veining, followed by quartz-K feldspar alteration (biotite and texture destroyed) with extreme cataclastic deformation. Where West porphyry and fine-grained porphyry fit in is not clear, but they too are cut by early-stage quartz veins and potassic alteration. The lack of observed intrusive contacts with truncated early-stage quartz veins and potassic alteration features prevents our interpreting with any confidence the potassic alteration as contemporaneous with one or more of the porphyries, as is typical of most other deposits. Before or at the onset of quartz-K feldspar alteration, and linked to the cataclastic deformation, there was local albitization, which may or may not be related to potassic alteration. Also not yet clear is the timing of quartz-K feldspar development relative to formation of quartz-molybdenite veins.

One of the major questions here is how much mineralization was emplaced during early stages of alteration. Early-stage quartz veins typically contain little more than trace sulfide, outside of clearly younger fractures. The quartz is, however, almost everywhere thoroughly recrystallized by younger events, which liberated any fluids trapped in early fluid inclusions and could have remobilized any original sulfide. Even though the quartz-K feldspar zone is the locus of the bornite-digenite center of the premain hydrothermal stage sulfide zoning pattern, most of the sulfide fills brittle fractures, which are clearly younger than the quartz-K feldspar alteration itself. In quartz-K feldspar rock lacking such fractures, disseminated sulfide, which is most likely to have been fixed with the alteration, is sparse. Also, this central sulfide assemblage commonly includes coarse-grained covellite with digenite, an association that characterizes the late-stage assemblage here but is not reported in deep central zones of other porphyry copper deposits. Nonetheless, the gradational decrease of Cu-Fe in the background sulfides eastward (and westward prior to the main stage), with pyrite appearing outside of sericitic veins and halos only after bornite disappears, and the disseminated to veinlet textures are typical of standard porphyry copper zoning. A complex history of introduction and remobilization of copper during the early stage is suggested. To help resolve this dilemma, it may be possible to date K feldspar and/or green sericite in quartz-K feldspar alteration with Ar-Ar techniques or possibly the bornite-digenite itself with Re-Os isotopes.

Main stage: The complexity of superimposed vein stages, complicated further by strong supergene effects, make it very difficult to decipher the individual evolutionary events and evaluate how much of the copper was actually introduced in each. Particularly, how much of the copper was introduced in

the early stage but remobilized in the main stage is an open question. Brimhall (1979, 1980) and Brimhall and Ghiorso (1983) have documented and thermodynamically modeled the hypogene leaching of early deep mineralization at Butte, Montana. This could have been accomplished and overlying main-stage veins formed by heated meteoric ground water, driven by intrusive dikes that also provided magmatic sulfur and arsenic. This phenomenon has clearly been operative at El Salvador, where early-stage chalcopyrite-bornite has been leached from deep pyritic D vein halos and reprecipitated higher up in pyrite-bornite assemblages (Gustafson and Hunt, 1975). Barren pyrite roots are typical of the Butte veins, and barren pyrite is the first sulfide formed in Brimhall's (1980) models. The pervasive deformation and recrystallization of early quartz veins at Chuquicamata, along with the low sulfide content of these veins and most potassic-altered rock (ignoring main-stage assemblages in later structures), suggests that much of the early-formed mineralization may have been remobilized. This copper could have been reprecipitated in main-stage veins. This would have required a magmatic source of heat and sulfur vapor. No intrusion of this age has been recognized, unless it is represented by the dike shown in Figure 3D.

The apparent paucity of pyrophyllite and dickite with the high-sulfidation assemblages of the last phases of this stage is unusual and suggests temperatures were too low to alter the previously formed sericite.

Late stage: The upward and eastward flaring of coarse-grained covellite was formed probably during both main and late stages, although distinction between the main and late stages is uncertain. The pattern correlates with increased sericitic overprinting of potassic alteration (Fig. 6A and B) and represents an upward zonation, which is here less structurally focused than in the quartz-sericite zone. It is also where coarse covellite-digenite without pyrite is abundant and where the sphalerite rims are most abundant and thickest. The sharp top of Zn values against the base of the supergene chalcocite blanket, the pattern of sphalerite rims in a parallel zone adjacent and below the chalcocite blanket, and their microscopic textures all argue for a supergene enrichment origin of the sphalerite rims (Aracena et al., 1997). However, their ubiquitous association with inner rims of coarse-grained covellite-digenite suggests formation in the late stage. Anhydrite in the late coarse-grained covellite veinlets confirms their formation above the temperature stability limit of gypsum, at least 55°C (Holland and Malinin, 1979), but the association with apparently amorphous hematite (Fig. 4E) argues against a much higher temperature. Furthermore, supergene sphalerite has never been reported in porphyry copper deposits, indicating that very unusual conditions would have prevailed here if this sphalerite were supergene. Normally Zn is so soluble in supergene solutions that it is completely lost from oxidizing orebodies unless precipitated as carbonates or sulfates. Here, however, an extraordinarily high sulfur activity was present to produce covellite. Lacking observation of sphalerite rims within anhydrite saturated rock, we cannot confidently link these with the late-stage covellite. However, if there had been a gradational waning of main-stage hydrothermal activity, with sulfur emanations continuing beyond the cutoff of copper and oxidizing, acid hot

spring activity above, we would have a mechanism for formation of all of the features we observe (L. Gustafson, unpub. report, 1994). These features include the gradational textures of not only covellite but also alunite, from coarse birefringent crystals typical of epithermal alteration to fine salt and pepper texture typical of supergene alteration. The dying stages of the hydrothermal system could have been very oxidizing, resulting in copper and zinc mobilized downward to be fixed as sulfide by reaction with the last emanations of reduced sulfur from below. Such an environment is speculated to have existed at El Salvador (Gustafson and Hunt, 1975; Gustafson et al., 2001) and evidence similar to that at El Salvador has been seen but not thoroughly followed up at Chuquicamata (Gustafson, unpub. report, 1993). Coarse-grained jarosite (in D1925), clearly derived instead of the expected hematitic limonite (Anderson, 1982) by oxidation of enriched chalcocite-pyrite, contains minute fluid inclusions with vapor bubbles. More work is needed.

Depth and timing: The coarse texture of the dominant East porphyry host rock and ductile deformation of early alteration minerals and veins, as well as stylolites in quartz-molybdenite veins, suggest deep emplacement. The finer grained porphyries are also strongly deformed. However, given the dynamic structural environment, and the fact that heat and rate of strain as well as pressure control the ductile-brittle transition in rocks, it is impossible to estimate depth of formation of these events. Early mineralization and alteration was most likely related to one or more of the smaller porphyry units that probably intrude East porphyry. Later main-stage hydrothermal veins in brittle fractures and with high-sulfidation assemblages more typical of epithermal environments look like much shallower features strongly telescoped on the earlier features. Zentilli et al. (1995) noted that the fission track study of Maksaev (1990) indicated that the Cordillera Domeyko underwent cooling due to rapid uplift and at least 4 to 5 km of erosion preceding 36 to 40 Ma but has been little eroded since 30 Ma, and that their Ar-Ar dating of East porphyry indicated intrusion as early as 35 Ma. This led them to the conclusion of at least two discrete hydrothermal pulses and erosion of the top of the early mineralized system before the onset of the second pulse. This is still an attractive hypothesis, but we recognize that it is based on too few facts. Much firmer geochronology of the intrusive units and alteration stages, supported by detailed observation of temporal relationships at intrusive contacts and crosscutting veins, is required to confirm or modify the hypothesis.

The questions of how much of the orebody was displaced by the West fault, and where it has gone, have intrigued explorationists for more than 50 yr and are argued still. The north-northeast elongate pattern of early potassic alteration does appear at depth to be truncated over more than 2 km, suggesting that much of the early-stage mineralization was lost by faulting, possibly displaced initially to the north. The much younger patterns of As and Zn (Figs. 7D and 8C) appear to be closing as they approach the West fault and they, too, have formed at least partly under the influence of this structure. This suggests there has been much less displacement of later main-stage mineralization and supergene enrichment than of early stages.

Comparison to other deposits

Chuquicamata clearly belongs to the broad class of porphyry copper deposits. It is part of a chain of classic Cu-Mo porphyry systems, formed during the Eocene-Oligocene, and which exhibit the typical range of porphyry copper characteristics. These are intimate space-time relationships with porphyritic intrusions, an evolution of zoned alteration-mineralization features, linked to structural evolution from ductile to brittle environments attending cooling of the host porphyries. But Chuquicamata is unique not only in its size and dynamism of its structural setting but also in several other features. It is more similar to Butte, Montana, than to most other porphyry copper deposits, and indeed it is this similarity that attracted Reno Sales and Anaconda to the property initially. The Rosario orebody at Collahuasi, with its late pyrite-enargite and bornite-tennantite veins, can also be compared to both Butte and Chuquicamata. This comparison was an important argument behind the initial discovery drilling campaign at Rosario (Hunt, 1985).

The presence of at least two hydrothermal events separated by a few million years is unusual but certainly not unique. Butte appears to have two distinctly separate mineralizing events, with main-stage veining superimposed on and above premain-stage mineralization, possibly 4 m.y. later (Meyer et al., 1968), but this too has proven to be a very challenging dating problem (Martin et al., 1999; Snee et al., 1999). El Salvador, Chile, has had two distinct periods of igneous activity, producing multiple and partially superimposed centers of mineralization separated by apparently 3 m.y. (Gustafson et al., 2001). Potrerillos (Marsh et al., 1997) is an example of a porphyry copper district with more widely spaced but largely nonoverlapping centers of intrusion and mineralization.

Hydrothermal breccias, present in greater or lesser abundance in most other porphyry deposits, are practically absent at Chuquicamata (the extensive brecciation in the quartz-sericite zone is mechanical brecciation related to the West fault). A contributing factor to this lack of brecciation may be the pervasive shattering of the rock at all stages of development of the orebody, which probably would have prevented buildup of excessive fluid pressure required for hydrothermal brecciation. This dynamic structural environment is also partly responsible for the abundance of veinlets and crackle-filling relative to more disseminated mineralization.

Chuquicamata shares with several other large deposits in the south-central Andean belt a tectonic setting and history conducive to formation of large porphyry coppers. Chuquicamata's position immediately within a major, long-lived, and very dynamic regional fault zone, which focused hydrothermal activity at least intermittently over millions of years, is almost surely the major reason why this deposit became such a huge concentration of metal and sulfur. This is also the reason it developed its many unique characteristics and then became segmented by postmineral faulting. Recent Re-Os isotope work by Mathur et al. (2000) suggests that Chuquicamata had a deeper sampling of more primitive magmas than other smaller Chilean porphyry copper deposits.

Conclusions

Chuquicamata is both the world's greatest copper orebody and the most unusual of all porphyry copper deposits. Much

has been learned about this phenomenal ore deposit, but there is a great deal we do not understand and much more to be done. The greatest challenges for geology at Chuquicamata are to point the way to discovery of all the higher grade oxide and sulfide ore still lying hidden in the district to sustain ongoing production and to define accurately the distribution, grade, rock mechanical and metallurgical characteristics of ore so as to optimize planning, mining, and metallurgical operations. The geologic documentation required for operational support, aided by a few critical academic studies, has produced the present level of understanding, and in one way or another, all of this knowledge aids those involved in the practical challenges just cited. It is a never-ending task and we still have a long way to go.

Acknowledgments

Although the authors assume full responsibility for the interpretations and conclusions presented here, we gratefully acknowledge the critical contributions of many others. Hundreds of man years of geologic effort, during both Anaconda's and CODELCO's tenure, have accumulated over the 84 yr of open-pit operation, and only a few of these people have been acknowledged by direct reference. The more recent contributions to the knowledge of Chuquicamata during the past 5 yr derives in large part from the major effort initiated under the leadership of Guillermo Ossandón and continued under Roberto Fréaut, as Superintendents of Geology at Chuquicamata. Major contributions during this period were made by the mine staff, particularly Irene Aracena, José Luis Fuenzalida, Darryl Lindsay, Victoriano Moyano, Fernando Ramírez, and José Rojas; by consultants William Chavez, Jr., Enrique Grez, Heinz Gröpper, Lewis Gustafson, Anthony Mayne-Nichols, Manuel Reyes, Sergio Vicencio, and Marcos Zentilli; and by Pedro Carrasco, Guillermo Müller, and Enrique Tidy of CODELCO Central. Regional geologic mapping by SERNAMEGOMIN was initiated at the request of Francisco Camus, Manager of Exploration for CODELCO. Gustafson drafted the present report. Very helpful reviews of the manuscript were provided by John Hunt, Marco Einaudi, Andrew Tomlinson, William Chavez, Jr., and John Dilles, but they bear no responsibility for any errors and misconceptions which may remain. Important financial and moral support and permission to publish were provided by the management of CODELCO in Chuquicamata and Santiago. CODELCO and *Economic Geology* underwrote the cost of color illustrations.

REFERENCES

- Ambrus, J., 1979, Emplazamiento y mineralización de los pórfidos cupríferos de Chile: Unpublished Ph.D. thesis, Salamanca, Spain, Universidad de Salamanca, 308 p.
- Anderson, J.A., 1982, Characteristics of leached capping and techniques of appraisal, in Titley, S.R., ed., *Advances in the geology of porphyry copper deposits, southwestern North America*: Tucson, University of Arizona Press, p. 275–295.
- Aracena, I., Ossandón C., G., and Zentilli, M., 1997, Mineralogía y distribución de Zinc en Chuquicamata: Enriquecimiento supergénico de Zinc?: Congreso Geológico Chileno, VIII, Antofagasta, v. III, p. 1908–1912.
- Alvarez, O., Miranda, J., and Guzmán, P., 1980, Geología del complejo Chuquicamata: Instituto de Ingenieros Minas de Chile, Santiago, v. 2, p. 314–363.
- Alvarez, C., and Flores, V., 1985, Alteración y mineralización hipógena en el yacimiento Chuquicamata, Chile: Congreso Geológico Chileno, IV, Antofagasta, v. 2, p. 78–100.

- Boric, P., Diaz, F., Makshev, V., 1990, Geología y yacimientos metalíferos de la region de Antofagasta: Santiago, Chile, Servicio Nacional de Geología y Minería-Chile, Bull. no. 40.
- Brimhall, G.H., Jr., 1979, Lithologic determination of mass transfer mechanisms of multiple-stage porphyry copper mineralization at Butte, Montana: Vein formation by hypogene leaching and enrichment of potassium-silicate protore: *Economic Geology*, v. 74, p. 555–589.
- 1980, Deep hypogene oxidation of porphyry copper potassium-silicate protore at Butte, Montana: A theoretical evaluation of the copper remobilization hypothesis: *ECONOMIC GEOLOGY*, v. 75, p. 384–409.
- Brimhall, G.H., Jr., and Ghiorso, M.S., 1983, Origin and ore-forming consequences of the advanced argillic alteration process in hypogene environments by magmatic gas contamination of meteoric fluids: *ECONOMIC GEOLOGY*, v. 78, p. 73–90.
- Chile Copper Company, 1917, First annual report: New York.
- Cuadra, P., and Rojas, G., 2001, Oxide mineralization at the Radomiro Tomic porphyry copper deposit, northern Chile: *ECONOMIC GEOLOGY*, v. 96, p. 387–400.
- Cuadra, P., Grez, E., and Gröpper, H., 1997, Geología del yacimiento Radomiro Tomic: Congreso Geológico Chileno, VIII, Antofagasta, v. III, p. 1918–1922.
- Dilles, J., Tomlinson, A., Martin, M., and Blanco, N., 1997, El Abra and Fortuna complexes: A porphyry copper batholith sinistrally displaced by the Falla Oeste: Congreso Geológico Chileno, VIII, Antofagasta, v. III, p. 1883–1887.
- Fam, R., and Rojas, O., 1997, Eventos de mineralización Exótica de Cu en el distrito de Chuquicamata, II region Chile: Congreso Geológico Chileno, VIII, Antofagasta, v. III, p. 1923–1927.
- Flores, R., 1985, Control del enriquecimiento supérgeno en el yacimiento Chuquicamata, Chile: Congreso Geológico Chileno, 4th, Antofagasta, Chile, Actas, v. 3, p. 228–249.
- Fréaut, R., Ossandón, G., and Gustafson, L.B., 1997, Modelo Geológico de Chuquicamata: Congreso Geológico Chileno, VIII, Antofagasta, v. III, p. 1898–1902.
- Gustafson, L.B., and Hunt, J.P., 1975, The porphyry copper deposit at El Salvador, Chile: *ECONOMIC GEOLOGY*, v. 70, p. 857–912.
- Gustafson, L.B., Orquera, W., McWilliams, M., Castro, M., Olivares, O., Rojas, G., Maluenda, J., and Mendez, M., 2001, Multiple centers of mineralization in the Indio Muerto district, El Salvador, Chile: *ECONOMIC GEOLOGY*, v. 96, p. 325–350.
- Holland, H.D., and Malinin, S.D., 1979, The solubility and occurrence of non-ore minerals, in Barnes, H.L., ed., *Geochemistry of hydrothermal ore deposits*, 2nd ed.: New York, NY, J. Wiley, p. 461–508.
- Hunt, J.P., 1969, Anhydrite and gypsum mineralization in porphyry copper deposits: Unpublished paper presented to the Penrose Conference at Tucson, Arizona, 22 p.
- 1985, Applied geology at Quebrada Blanca and Collahuasi, Chile, and in the future of U.S. metal mining: *ECONOMIC GEOLOGY*, v. 80, p. 794–800.
- Jarrell, O.W., 1944, Oxidation at Chuquicamata, Chile: *ECONOMIC GEOLOGY*, v. 39, p. 251–286.
- Lewis, M., 1996, Characterization of hypogene covellite assemblages at the Chuquicamata porphyry copper deposit, Chile, section 4500N: Unpublished M.Sc. thesis, Halifax, NS, Dalhousie University, 223 p.
- Lindsay, D.D., 1998, Structural control and anisotropy of mineralization in the Chuquicamata porphyry deposit, Chile: Unpublished Ph.D. thesis, Halifax, NS, Dalhousie University, 381 p.
- Lindsay, D., Zentilli, M., and Rojas, J., 1995, Evolution of an active ductile to brittle shear system controlling mineralization at the Chuquicamata porphyry copper deposit, northern Chile: *International Geology Review*, v. 37, p. 945–958.
- Lira, G., 1989, Geología del area preandina de Calama, con énfasis en la estratigrafía y paleogeografía del Mesozoico, 22 a 24 40' latitud sur, región de Antofagasta, Chile: Memoria de Título, Universidad de Chile, Departamento de Geología y Geofísica, 233 p.
- López, V.M., 1939, The primary mineralization at Chuquicamata, Chile, S.A.: *ECONOMIC GEOLOGY*, v. 34, p. 674–711.
- 1942, Chuquicamata, Chile, in Newhouse, W.H., *Ore deposits as related to structural features*: Princeton, NJ, Princeton University Press, p. 126–128.
- Makshev, V., 1990, Metallogeny, geological evolution, and thermochronology of the Chilean Andes between latitudes 21°N and 21°S and the origin of major porphyry copper deposits: Unpublished Ph.D. thesis, Halifax, NS, Dalhousie University, 553 p.
- Makshev, V., and Zentilli, M., 1988, Marco metalogénico regional de los megadepósitos de tipo pórfido cuprífero del norte grande de Chile: Congreso Geológico Chileno, V, Santiago, v. I, p. B131–B133.
- 1999, Fission track thermochronology of the Domeyko Cordillera, northern Chile: Implications for Andean tectonics and porphyry copper metallogenesis: *Exploration and Mining Geology*, v. 8, p. 65–88.
- Makshev, V., Zentilli, M., and Reynolds, P.H., 1988, ⁴⁰Ar/³⁹Ar geochronology of porphyry copper deposits of the northern Chilean Andes: Congreso Geológico Chileno, V, Santiago, v. I, p. B109–B131.
- Marinovic, S., and Lahsen, N., 1984, Region de Antofagasta: Santiago, Chile, Instituto de Investigaciones Geológicas, scale 1:250,000.
- Marsh, T.M., Einaudi, M.T., and McWilliams, M., 1997, ⁴⁰Ar/³⁹Ar geochronology of Cu-Au and Au-Ag mineralization in the Potrerillos district, Chile: *ECONOMIC GEOLOGY*, v. 92, p. 784–806.
- Martin, M.W., Dilles, J.H., and Proffett, J.M., 1999, U-Pb geochronologic constraints for the Butte porphyry system [abs.]: Geological Society of America Abstracts with Program, Abstract 51723, v. 31, p. A-380.
- Mathur, R., Ruiz, J., and Munizaga, F., 2000, Relationship between copper tonnage of Chilean base metal porphyry deposits and Os isotope ratios: *Geology*, v. 28, p. 555–558.
- Meyer, C., Shea, E.P., Goddard, C.C., Jr, and staff, 1968, Ore deposits of Butte, Montana, in Ridge, J.D., ed., *Ore Deposits of the United states, 1933–1967*: New York, AIME.
- Miller, B.L., and Singewald, J.T., Jr., 1919, The mineral deposits of South America: New York, McGraw Hill.
- Mortimer, C., Munchmeyer F. C., and Urqueta D., I., 1977, Emplacement of the Exótica orebody, Chile: Institute of Mining and Metallurgy Transactions, sec. B, v. 86, p. B121–B127.
- Mpodozis, C., Marinovic, N., Smoje, I., and Cuitiño, L., 1993, Estudio Geológico-estructural de la Cordillera de Domeyko entre Sierra Limón Verde y Sierra Mariposas, region de Antofagasta: Servicio Nacional de Geología y Minería-CODELCO Report IR-93-04, 282 p.
- Munchmeyer, C., 1996, Exotic deposits—products of lateral migration of supergene solutions from porphyry copper deposits: Society of Economic Geologists Special Publication 5, p. 43–58.
- Newberg, D.W., 1967, Geochemical implications of chrysocolla-bearing alluvial gravels: *ECONOMIC GEOLOGY*, v. 62, p. 932–956.
- Ossandón C., G., and Zentilli, M., 1997, El distrito de Chuquicamata: una concentración de cobre de clase mundial: Congreso Geológico Chileno, VIII, Antofagasta, v. III, p. 1888–1892.
- Perry, V.D., 1952, Geology of the Chuquicamata orebody: *Mining Engineering*, December, p. 1166–1168.
- Quinteros, L., 1997, La Digenita y su asociación con covelina en la zona de alteración potásica, al este del sistema de la falla Americana: Congreso Geológico Chileno, VIII, Antofagasta, v. III, p. 1958–1965.
- Quinteros, L., and Fréaut, R., 1997, La distribución del molibdeno en el yacimiento de Chuquicamata: Congreso Geológico Chileno, VIII, Antofagasta, v. III, p. 1903–1907.
- Reynolds, P., Ravenhurst, C., Zentilli, M., and Lindsay, D., 1998, High-precision ⁴⁰Ar/³⁹Ar dating of two consecutive hydrothermal events in the Chuquicamata porphyry copper system, Chile: *Chemical Geology*, v. 148, p. 45–60.
- Renzi, B., 1957, Geology and petrogenesis at Chuquicamata, Chile: Unpublished Ph.D. thesis, Bloomington, IN, Indiana University, 71 p.
- Reutter, K-J, Chong, G., and Scheuber, E., 1993, The West Fissure and the Precordilleran fault system of northern Chile [ext. abs.]: Andean Geodynamics, International Symposium, 3rd, Oxford, UK, September 21–23, 1999, ORSTOM-University of Oxford, Extended Abstracts, p. 237–240.
- Rojas, J., and Lindsay, D., 1997, Evaluación estructural de Chuquicamata, su relación con la intrusión del pórfido y eventos de alteración y mineralización: Congreso Geológico Chileno, VIII, Antofagasta, v. III, p. 1893–1897.
- Sillitoe, R.H., 1988, Epochs of intrusion-related copper mineralization in the Andes: *Journal of South American Earth Sciences*, v. 1, p. 89–104.
- Sillitoe, R.H., and McKee, E.H., 1996, Age of supergene oxidation and enrichment in the Chilean porphyry copper province: *ECONOMIC GEOLOGY*, v. 91, p. 164–179.
- Snee, I., Miggins, D., Geissman, J., Reed, M., Dilles, J., and Zhang, L., 1999, Thermal history of the Butte porphyry system, Montana [abs.]: Geological Society of America Abstracts with Program, Abstract 50611, v. 31, p. A-380.
- Society of Economic Geologists, 1997, Congreso Geológico Chileno, 8th, Universidad Católica del Norte, v. 3, p. 1871–1965.

- Soto, H., 1979, Alteración y mineralización primaria en Chuquicamata: Unpublished Ph.D. thesis, Salamanca, Spain, Universidad de Salamanca, 233 p.
- Stoffgren, R.E., and Alpers, C.N., 1987, Svanbergite and woodhouseite in hydrothermal ore deposits: Implications for apatite destruction during advanced argillic alteration: *Canadian Mineralogist*, v. 25, p. 201–212.
- Taylor, A.V., Jr., 1935, Ore deposits of Chuquicamata, Chile: *International Geological Congress*, 16th, Washington, DC, Proceedings, v. 2, p. 473–484.
- Tomlinson, A., and Blanco, N., 1997, Structural evolution and displacement history of the West fault system, Precordillera, Chile: Part 1. Premineral history. Part 2. Synmineral history: *Congreso Geológico Chileno*, VIII, Antofagasta, v. III, p. 1873–1882.
- Torres, R., Flores, G., and Suárez, S., 1997, Caracterización Geotécnica mina Chuquicamata: *Congreso Geológico Chileno*, VIII, Antofagasta, v. III, p. 1938–1942.
- Vega, M., 1991, Estudios de inclusiones fluidas en el sector norte del yacimiento Chuquicamata, Región de Antofagasta Chile [abs.]: *Congreso Geológico Chileno*, VI, Viña del Mar, Chile, Extended Abstracts, v. I, p. 390–393.
- Zentilli, M., Graves, M., Lindsay, D., Ossandón, G., and Camus, F., 1995, Recurrent mineralization in the Chuquicamata porphyry copper system: Restrictions on genesis from mineralogical, geochronological and isotopic studies, in Clark, A.H., ed., *Proceedings, Giant ore deposits II workshop*: Kingston, ON, Queens University, p. 86–100 (second, corrected printing, p. 90–113).